

CHAPTER 4

RESULTS AND DISCUSSION

1. Extraction of plants

Twenty six plants were selected from their usage involving in hair treatment and/or their phytochemical constituents. Ethyl alcohol was used as the extraction solvent in this experiment due to its semi-polar property. Using the semi-polar solvent for extracting suspected phytochemical classes (Table 2) which could inhibit 5 α R enzyme may be better than other organic solvents. In addition, safety of ethanol extract is higher than any of other organic solvents. Moreover, the compatibility between ethanolic extract and compositions in cosmetic formulations are better than any of those organic solvents. Extraction yields of these plants are shown in Table 3.

Table 3 Extraction yields of the plants

Family	Scientific name	Part used	% yield
Acanthaceae	<i>Rhinacanthus nasutus</i> Kuntze	Leaves	4.60
	<i>Andrographis paniculata</i> Nees	Stems	2.94
Apiaceae	<i>Centella asiatica</i> (L.) Urb.	Leaves	10.26
Caesalpinaceae	<i>Cassia siamea</i> Lam.	Leaves	2.18
Combretaceae	<i>Terminalia chebula</i> Retz.	Fruits	11.50

Table 3 (continued)

Family	Scientific name	Part used	% yield
Combretaceae	<i>Terminalia bellirica</i> (Geartn.) Roxb.	Fruits	16.05
Compositae	<i>Carthamus tinctorius</i> L.	Florets	19.25
Convovulaceae	<i>Ipomoea aquatica</i> Forssk.	Whole plants	1.90
Cucurbitaceae	<i>Trichosanthes cucumerina</i> L.	Fruits	2.75
Euphorbiaceae	<i>Phyllanthus emblica</i> L.	Fruits	21.63
Graminae	<i>Oryza sativa</i> L.	Grains	2.22
Guttiferae	<i>Garcinia magostana</i> L.	Fruit peels	14.78
Lamiaceae	<i>Ocimum bacilicum</i> L.	Leaves	2.74
Leguminosae	<i>Acacia concinna</i> Wall.	Pods	15.23
Lythraceae	<i>Lawsonia inermis</i> L.	Leaves	16.6
menispermaceae	<i>Tinospora rumphii</i> Boerl.	Whole plants	3.88
Oxalidaceae	<i>Averrhoa carambola</i> L.	Fruits	4.65
Papillionaceae	<i>Clitoria ternatea</i> L.	Flowers	18.61
Piperaceae	<i>Piper nigrum</i> Wall.	Fruits	13.60
Poaceae	<i>Cymbopogon citratus</i> Stapf	Whole plants	4.00
Rutaceae	<i>Citrus hystrix</i> DC.	Fruit peels	8.24
	<i>Citrus reticulata</i> Blanco	Fruit peels	14.06
Sapindaceae	<i>Sapindus rarak</i> DC.	Fruits	4.40
Zingiberaceae	<i>Zingiber officinale</i> Roscoe	Rhizomes	8.44
	<i>Alpinia galanga</i> Willd.	Rhizomes	5.88
	<i>Curcuma longa</i> L.	Rhizomes	7.84

From Table 3, the yields of extraction were ranged from 1.9 to 21.63 % of their fresh weight. *P. emblica* has the highest yield of extraction followed by *C. tinctorius* (19.25 %) and *C. ternatea* (18.61 %). *I. aquatica* has the lowest yield of extraction. All crude extract appeared as a hard semisolid extract.

2. Total phenolic content of plant extracts

Usually, the methods used to identify or to control the quality and strength of the plant extracts are chromatography techniques. For examples, thin layer chromatography (TLC) and high performance liquid chromatography (HPLC), by using the standard phytochemicals that are predominant in that kind of plants. However, these methods possessed some drawbacks such as high costs of the standards and difficulty in the finding of suitable chromatographic conditions. The analysis for total phenolic content (TPC) of these plants is a more preferable method since the analysis for TPC is rapid, simple and only has one universal condition for every kind of plant samples. Moreover, only one standard phenolic compound is needed. In this experiment, gallic acid was used as a standard. TPCs of the plants are shown in Table 4.

In an analysis of TPC (Table 4), there were five plants that contain only traces amount of phenolic compounds, which were *T. cucumerina*, *O. sativa*, *A. concinna*, *A. carambola*, and *S. rarak*. The TPC of other plants were ranged from 12.20 to 450.03 mg gallic acid equivalent/ g extract. *P. emblica* has the highest TPC, followed by *T. bellirica* (370.85) and *T. chebula* (286.94). TPC will be used as a simple quality control method for plant materials used.

Table 4 Total phenolic content of the extracts

Scientific name	Total phenolic content (mg GAE/ g extract)*
<i>Phyllanthus emblica</i> L.	450.03 ± 10.40a
<i>Terminalia bellirica</i> (Geartn.) Roxb.	370.85 ± 26.80b
<i>Terminalia chebula</i> Retz.	286.94 ± 3.37c
<i>Zingiber officinale</i> Roscoe	248.07 ± 14.16c
<i>Alpinia galanga</i> Willd.	228.54 ± 24.17c
<i>Curcuma longa</i> L.	218.26 ± 14.90c
<i>Garcinia magostana</i> L.	205.90 ± 6.05c
<i>Lawsonia inermis</i> L.	120.71 ± 3.01d
<i>Cassia siamea</i> Lam.	99.81 ± 0.31d
<i>Tinospora rumphii</i> Boerl.	83.64 ± 0.83d
<i>Citrus reticulata</i> Blanco	75.53 ± 5.46de
<i>Ocimum bacilicum</i> L.	63.12 ± 0.57e
<i>Ipomoea aquatica</i> Forssk.	61.95 ± 2.5e
<i>Piper nigrum</i> Wall.	60.75 ± 3.26ef
<i>Andrographis paniculata</i> Nees	46.19 ± 2.29f
<i>Citrus hystrix</i> DC.	34.43 ± 5.14f
<i>Centella asiatica</i> (L.) Urb.	32.00 ± 0.91f
<i>Carthamus tinctorius</i> L.	28.34 ± 0.57f
<i>Rhinacanthus nasutus</i> Kuntze	26.59 ± 2.11f
<i>Clitoria ternatea</i> L.	24.49 ± 2.76f

Table 4 (continued)

Scientific name	Total phenolic content (mg GAE/ g extract)
<i>Cymbopogon citratus</i> Stapf	12.20 ± 3.31g
<i>Oryza sativa</i> L.	< 10
<i>Trichosanthes cucumerina</i> L.	< 10
<i>Acacia concinna</i> Wall.	< 10
<i>Averrhoa carambola</i> L.	< 10
<i>Sapindus rarak</i> DC.	< 10

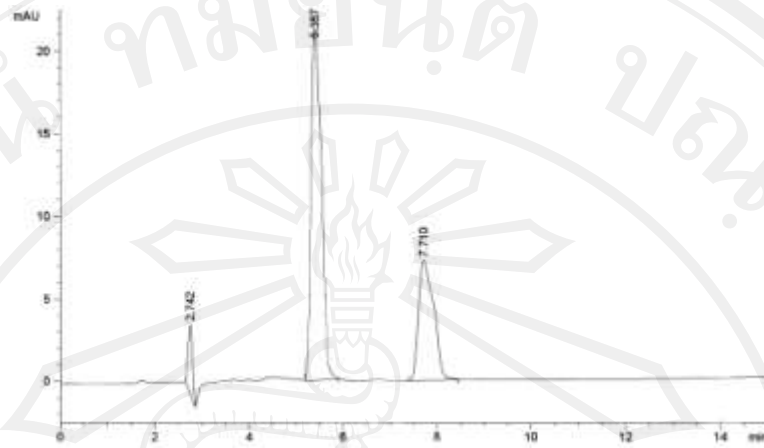
* Values in Table expressed as mean ± SD of triplicate experiments. Means in column with different letters are significantly different ($p < 0.05$).

3. 5 α -reductase inhibitory activity of the plant extracts

Normally, the assessment for the 5 α -reductase inhibitory activity, the complex methods such as radioimmunoassay (Park et al., 2003) and the chromatographic mass spectrometry (Li et al., 2009) were used. The radioimmunoassay method provides disadvantages because the use of dangerous radioactive compounds as the substrate and the requirements of complex protection and analysis equipment. The chromatographic mass spectrometry also requires the complex equipment. Since our facility cannot support these kinds of analyses, simple and rapid HPLC-UV was used in this study. Moreover, simple HPLC technique requires less instrumental and provide safer than radioimmunoassay technique.

For the 5α -reductase inhibitory activity, microsomal suspension from rat livers was used as an enzyme sources. After preparation, microsomal enzyme suspension appeared as a pink-opaque liquid with the soluble protein of 4.71 mg/ml, assessed by the Lowry method. Finasteride, the commercially available 5α -reductase inhibitor that FDA approved for treating androgen related disorders, was used as a standard enzyme inhibitor. Two distinctive reactions were constructed for controlling of the enzyme availability and activity. Firstly, the reaction control was the reaction that the enzyme from microsomal suspension gained it full activity (0% inhibition). Secondly, the enzyme blank was the reaction that the enzyme was forced to be denatured; thus no activity was occurred in this reaction (100% inhibition). After the analysis of remaining testosterone between these two reactions and in the reaction of any other substance, we can determine the ability of substance for enzyme inhibition. From given HPLC condition, testosterone and internal standard (propyl p-hydroxybenzoate) gave retention time at around 8 and 5 min, respectively. The HPLC chromatogram of the reaction control and enzyme blank are shown in Figure 8A and 8B, respectively. In these chromatograms, the peak at retention time around 2.5 min was determined to be a dithiothreitol. This compound was used in the method of enzyme preparation to preserve the reduction function of the enzyme. This peak was not be used in the calculation process.

A:



B:

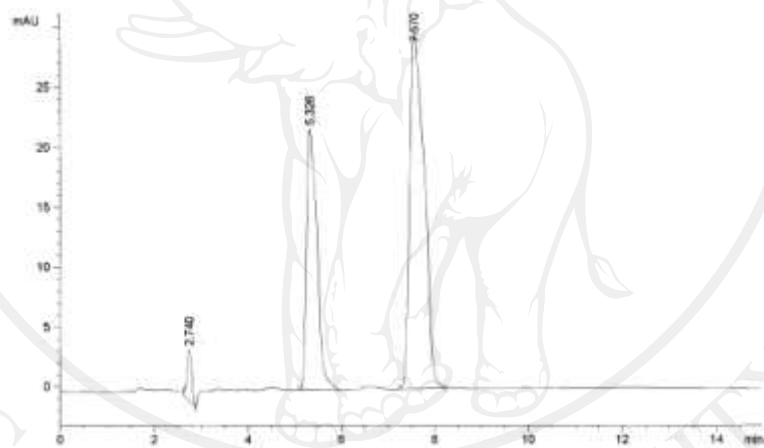


Figure 8 HPLC chromatogram of (A) reaction control which is the reaction that enzyme have full activity (0 % inhibition) and (B) enzyme blank which is the reaction that enzyme have no activity (100 % inhibition). Testosterone and internal standard gave retention time at around 8 and 5 min, respectively.

Figure 8A suggested that the full activity of the 5α -reductase converted substrate testosterone into the more active androgen dihydrotestosterone, which cannot be detected by UV absorption at this wavelength. This represented the remaining amount of testosterone that was occurred from conversion of the enzyme.

Comparing to Figure 8B, which enzyme have no activity, the peak of testosterone (at around 8 min) is higher than in 8A, this is the amount of the testosterone added in the reaction. The balance between peak area ratio of testosterone and internal standard in the reactions made us known the activity of that compound, which can be calculated by the given equation in chapter 3. An internal standard (propyl *p*-hydroxybenzoate, retention time at around 5 min) was used to ensure the viability of extraction processes.

HPLC chromatogram of the reaction containing 0.5 μM finasteride is shown in Figure 9.

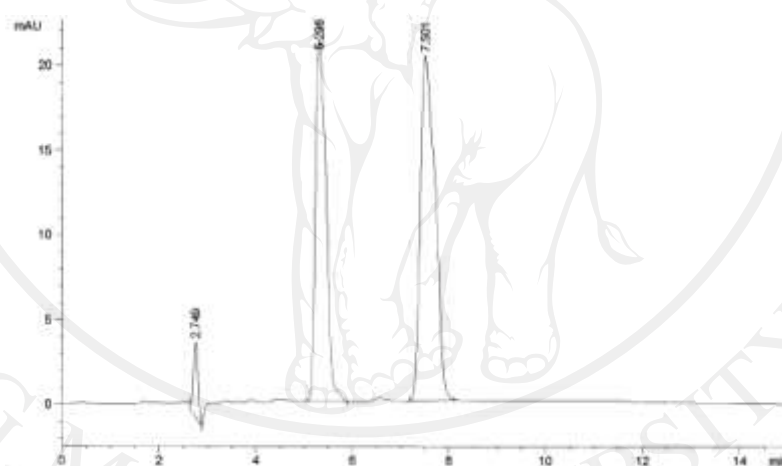


Figure 9 HPLC chromatogram of the reaction containing 0.5 μM finasteride. Testosterone and internal standard gave retention time at around 8 and 5 min, respectively.

Seen in Figure 9, the amount of remaining testosterone observed at the peak was nearly as the enzyme blank (Figure 8B).

Ten concentrations range of finasteride between 0.1 to 1.0 μM were studied, the standard curve for the 5α -reductase inhibiting was constructed. Linearity was

found only in concentration range between 0.1 to 0.5 μM , this range was used to construct the standard equation. The finasteride inhibition curve is shown in the Figure 10.

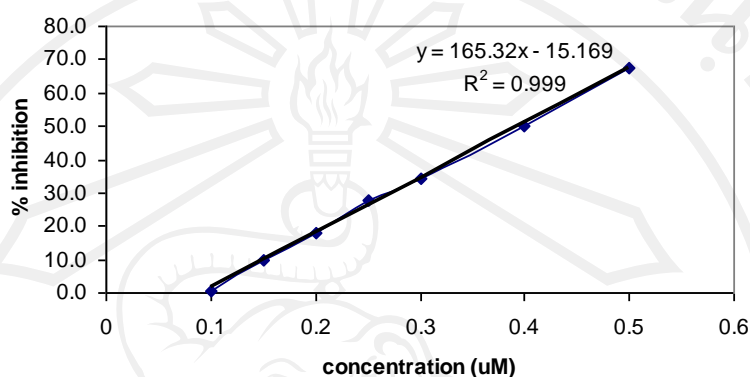


Figure 10 Finasteride inhibition curve

From Figure 10, finasteride gave IC_{50} at 0.394 μM , which was comparable to previously published result of 0.34 μM , reported by Park et al. (2003) which was analyzed by radioimmunoassay. Standard equation $y = 165.32x - 15.169$ was used for calculating the finasteride equivalent 5α -reductase inhibitory activity or FEA value, which expressed as mg finasteride equivalent per g extract. Using FEA value to compare the activity between the substances is easier than the IC_{50} . Moreover, in order to obtain IC_{50} , series of concentrations of compound are needed. FEA value is proportionally related to the $5\alpha\text{R}$ inhibitory activity, the higher the FEA value, the higher the $5\alpha\text{R}$ inhibitory activity. FEA values of selected plants are shown in the

Table 5.

Table 5 5 α -reductase inhibitory activity of the plant extracts

Scientific name	FEA value*
<i>Carthamus tinctorius</i> L.	24.67 \pm 1.74a
<i>Phyllanthus emblica</i> L.	19.25 \pm 0.44b
<i>Cymbopogon citratus</i> Stapf	19.03 \pm 0.15b
<i>Alpinia galanga</i> Willd.	18.95 \pm 0.93b
<i>Zingiber officinale</i> Roscoe	18.41 \pm 1.04bc
<i>Ocimum bacilicum</i> L.	17.59 \pm 1.00c
<i>Oryza sativa</i> L.	16.72 \pm 0.95c
<i>Clitoria ternatea</i> L.	15.34 \pm 1.30c
<i>Curcuma longa</i> L.	13.83 \pm 1.03d
<i>Centella asiatica</i> (L.) Urb.	13.73 \pm 1.05d
<i>Citrus hystrix</i> DC.	13.72 \pm 0.90d
<i>Trichosanthes cucumerina</i> L.	13.37 \pm 0.84d
<i>Tinospora rumphii</i> Boerl.	13.36 \pm 0.62d
<i>Ipomoea aquatica</i> Forssk.	13.16 \pm 0.43d
<i>Averrhoa carambola</i> L.	13.12 \pm 0.87d
<i>Andrographis paniculata</i> Nees	13.01 \pm 0.81d
<i>Cassia siamea</i> Lam.	12.87 \pm 1.12d
<i>Sapindus rarak</i> DC.	12.81 \pm 0.84d
<i>Acacia concinna</i> Wall.	12.78 \pm 0.87d
<i>Terminalia chebula</i> Retz.	12.74 \pm 0.84d
<i>Lawsonia inermis</i> L.	12.36 \pm 1.62d

Table 5 (Continued)

Scientific name	FEA value*
<i>Garcinia magostana</i> L.	11.62 ± 1.18d
<i>Terminalia bellirica</i> (Geartn.) Roxb.	11.58 ± 0.84d
<i>Piper nigrum</i> Wall.	11.18 ± 0.81d
<i>Rhinacanthus nasutus</i> Kuntze	10.79 ± 1.30d
<i>Citrus reticulata</i> Blanco	5.56 ± 1.12e

* FEA (Finasteride equivalent 5 α -reductase inhibitory activity) value reported as mean \pm SD of triplicate experiments. Mean in column with different letters are significantly different ($p < 0.05$).

From Table 5, the FEA values of tested compounds were ranged from 5.56 to 24.67 mg finasteride equivalent/g extract. *C. tinctorius* had the highest activity, followed by *P. emblica* (FEA = 19.25) and *C. citratus* (FEA = 19.03). The lowest activity was found in *C. reticulata*.

Pearson's correlation coefficient was used to determine the correlation between the TPC of the extract and the FEA value, but there was no any correlation between these parameters ($r = 0.104$, $p = 0.364$). The scatter plot between TPC and FEA value is shown in Figure 11.

Previous report suggested that polyphenol compounds can inhibit the 5 α R (Hiipakka et al., 2001). Since there is no relationship between the two parameters (Figure 11), other phytochemical classes in the plants may play an important role in the inhibition of the enzyme, or else the synergistic or antagonistic actions between

various phytochemical classes extracted from the plants may result in a different inhibitory activity. Further investigation is needed to confirm this reason.

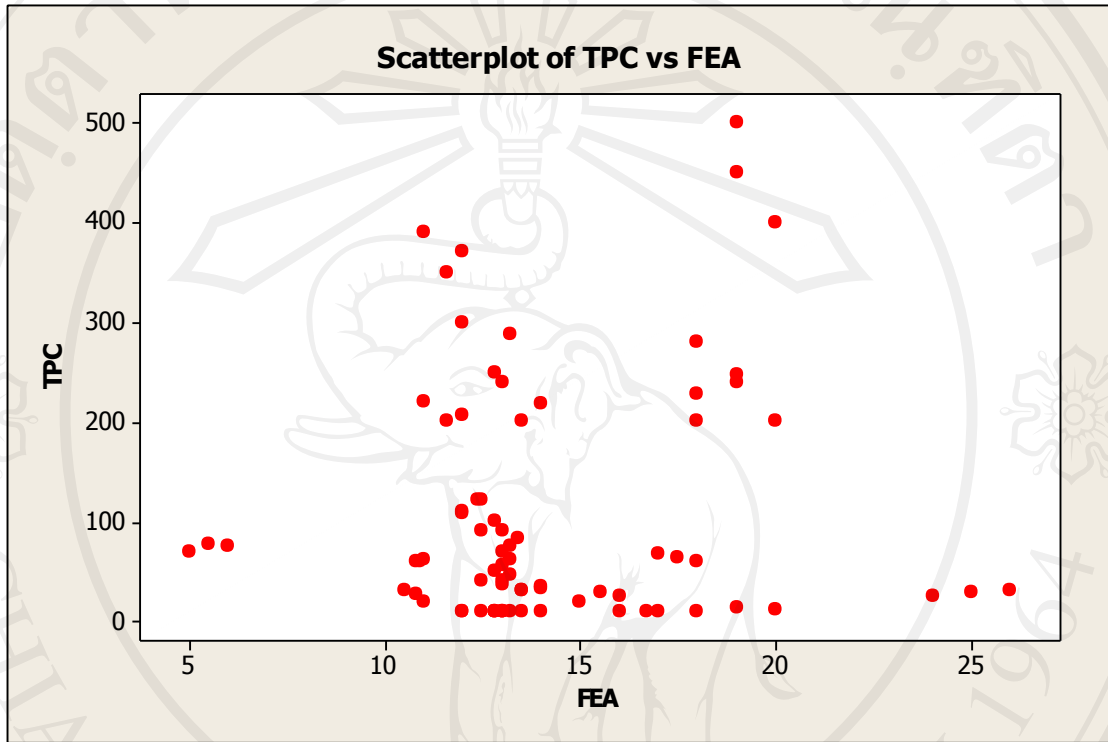


Figure 11 Scatter plot between FEA value and TPC, values are from 26 plants with 3 replicated experiments

In the confirmation of the activity of *C. tinctorius*, standard safflower yellow which is the most abundant phytochemical found in the florets was further tested by the same method. The IC_{50} of safflower yellow was 119.9 ppm (FEA value = 12.74). Since the activity of safflower yellow is only half of the extract itself, this suggested that synergistic action between other phytochemicals in the safflower extract may be a result in the higher FEA value of the standard.

Since there were no significant differences in 5 α R inhibitory activity among *P. emblica*, *C. citratus*, *A. galangal* and *Z. officinale* and among *Z. officinale*, *O. bacilicum*, *O. sativa*, and *C. ternatea*. *P. emblica* or emblica was selected as a second potent 5 α R inhibitor and *C. ternatea* or butterfly pea was selected as a third potent 5 α R inhibitor due to their frequent use in traditional herbals for treating hair loss.

The usual dosage of finasteride for the treatment of alopecia is 1 mg per day (Lacy et al., 2008), the data obtained from this study suggested that regular intake of these fresh plants or the extract may be useful in the treatment of the alopecia. Further investigation on the topical application of the plants that exert 5 α R inhibitory activity to treat hair loss and promote hair growth will be done in the next part of this work.

3. Hair growth promoting activity of plant extracts

Hair growth promoting activity of the top three extracts were tested in the C57BL/6Mlac mice model, using minoxidil as a positive control and vehicle made from propylene glycol, ethanol and water as a negative control. Containing no melanin in the dermal of C57BL/6 mice, the melanogenesis of these mice occurred only in the hair during the anagen phase of hair growth (Slominski, 1994). This reason makes the C57BL/6 mice become more interested in many hair growth researches. Especially, when these mice are grown to the seven-week-old, all of their hair follicles are in the telogen phase. When shaving mice at this period, the white skin is observed and will become black only when the anagen phase is re-initiated.

By given hair growth score ranging from 0 to 5 according to the percentage of the regrowth hair after shaving (Figure 7). Hair growth promoting effects of tested compounds are shown in the Figure 12.

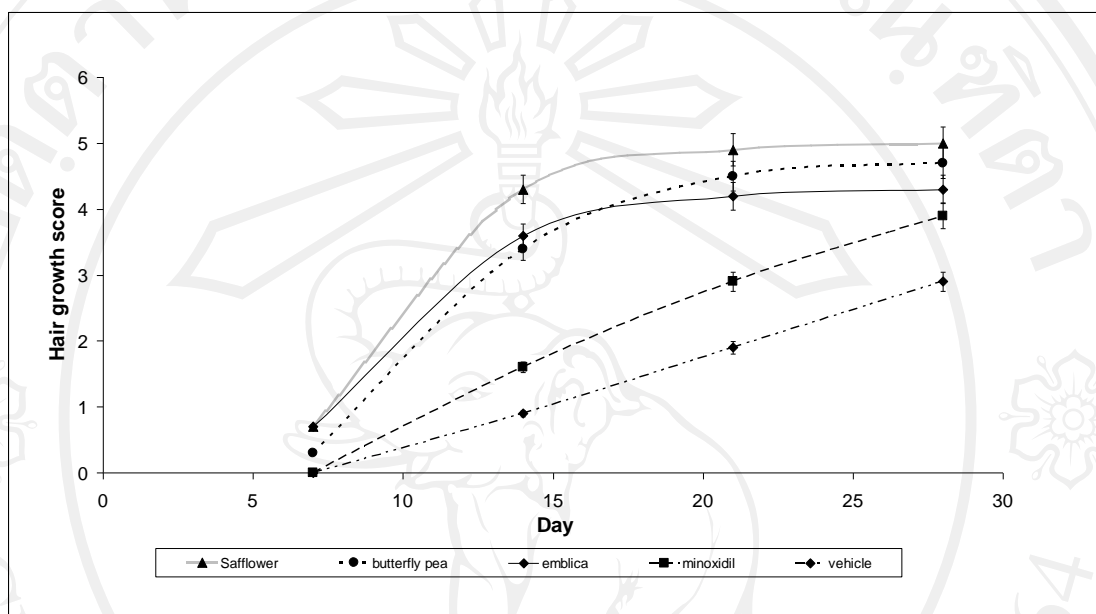


Figure 12 Hair growth promoting activity of safflower, butterfly pea, emblica, minoxidil and vehicle treated mice

From Figure 12, the normal hair growth rate of the mice was seen in the growth curve of vehicle. In the mice that received minoxidil, the slope of hair growth curve was greater than that of the vehicle, suggesting that minoxidil promoted hair growth rate. Hair growth of the mice received safflower was the highest, the hair of the mice was nearly full growth observed, while in the other group mostly hair were still no growth. In addition, safflower extract did promote hair growth better than minoxidil ($p < 0.05$) at day 28. All of the tested plant extracts tested did increase the hair growth rate during the first 14 days. On the latter days, a constant hair growth rate of the mice was observed in all of the three extracts groups.

The total hair growth of mice that received vehicle, minoxidil, safflower, butterfly pea and emblica extract, obtained from Coscam[®] on day 28, are shown in Figure 13A, 13B, 13C, 13D and 13E, respectively.

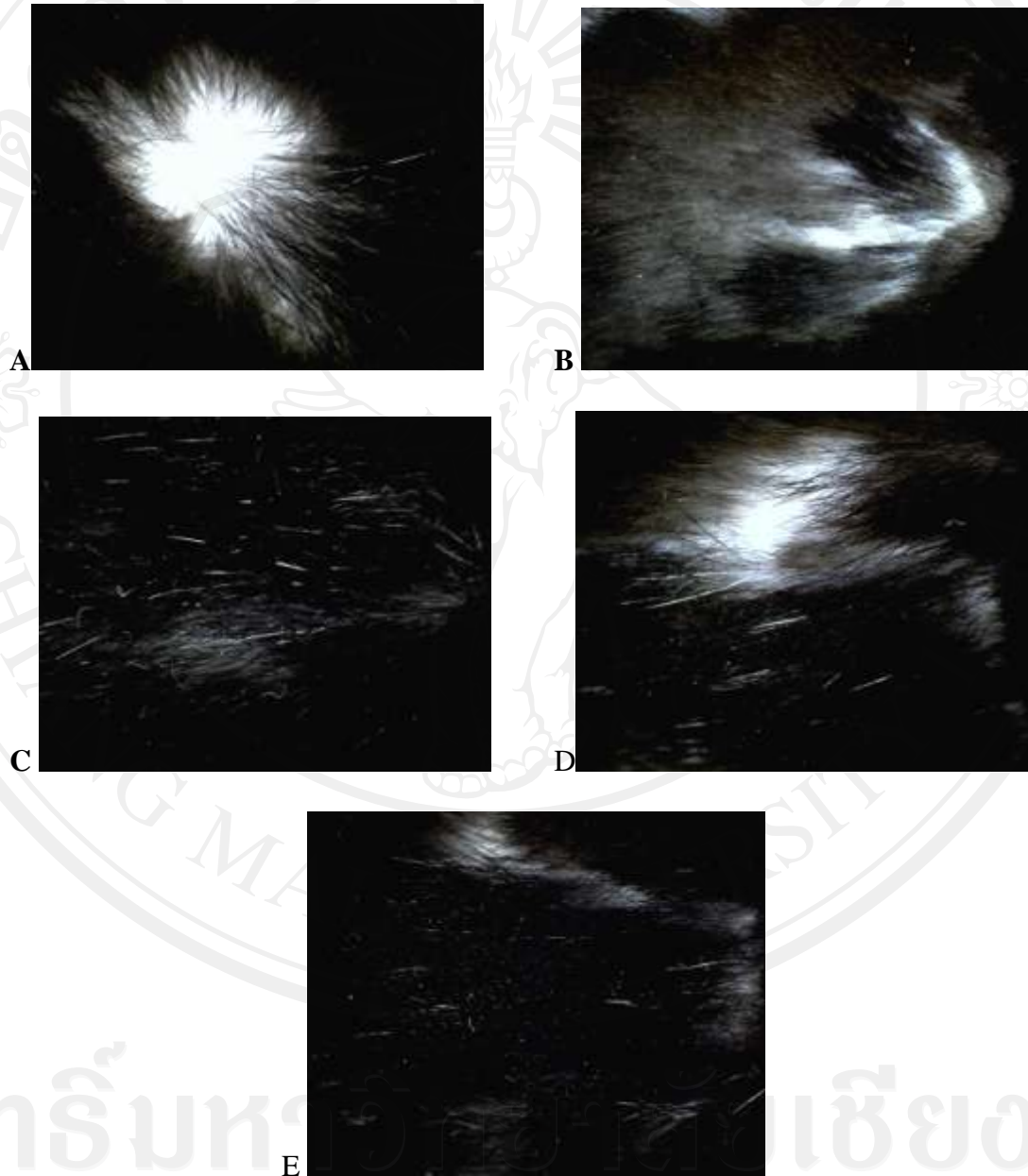


Figure 13 Total hair growth after day 28, digital images obtained from Coscam[®] USB-225 with 40x magnification lens: (A) vehicle (B) minoxidil and (C) safflower (D) butterfly pea and (E) emblica treated mice.

After imaging of total hair growth by using Coscam[®], the mice were sacrificed and their dorsal skins were removed and sectioned. The histological morphology of the hair follicles of the mice are shown in Figure 14.

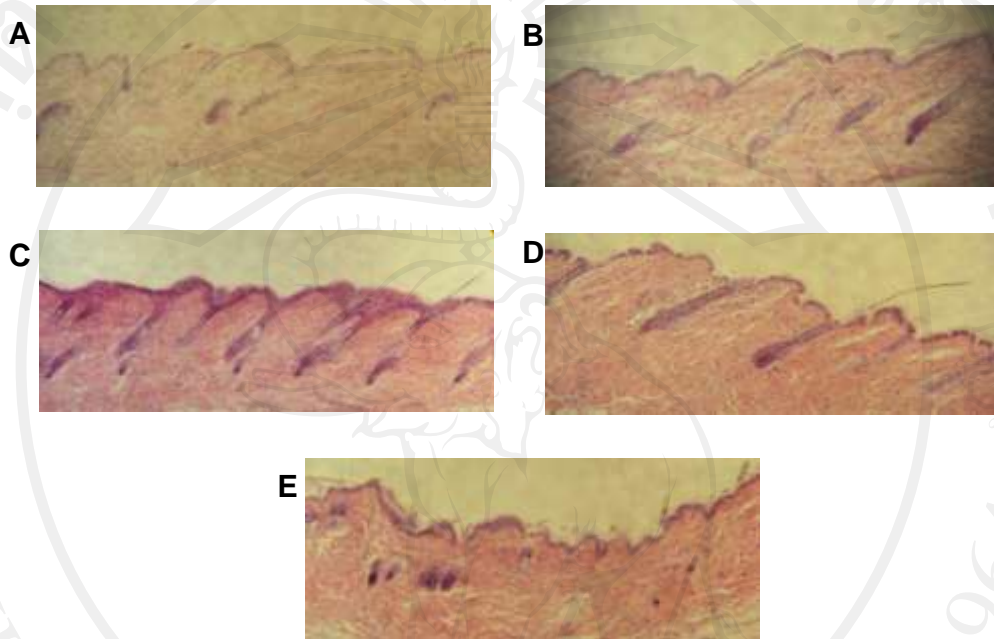


Figure 14 Hair follicle histological morphology of the mice received (A) vehicle (B) 2 % minoxidil (C) safflower extract (D) butterfly pea extract and (E) emblica extract. Digital images obtained from 100 × magnification of light microscope. (Kumar et al., 2012)

Figure 14 is the longitudinal section of the dorsal skin showing hair follicle unit and skin structure. The hair follicles of the mice received safflower were the densest, followed by butterfly pea and emblica. There was no difference in hair follicle between the mice received minoxidil or vehicle.

For confirmation, cross-sectional studied was performed to count the number of hair follicles in area under the light microscope, the example of cross sectioned skin of the mice received safflower extract is shown in Figure 15.

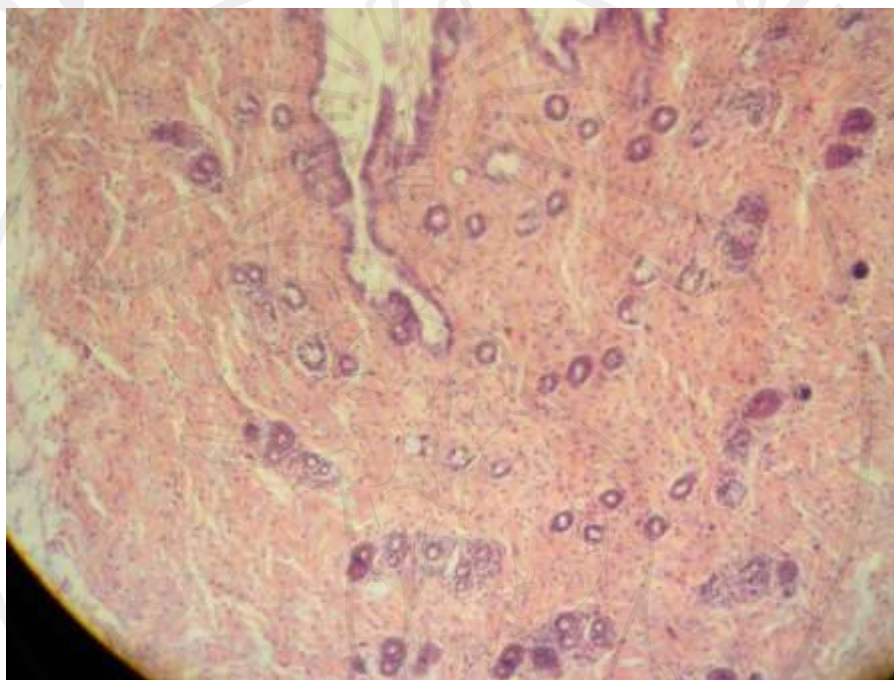


Figure 15 Cross-sectional studied of the dorsal skin of mice received safflower extract, showing hair follicle. Digital image obtained from $100\times$ magnification of light microscope.

From Figure 15, the hair follicle unit under cross-sectional appeared as the purple-red circle where one circle is one hair follicle unit. The mice received different tested compounds have shown a difference in hair follicle number. In this area of magnification under $100\times$ of the light microscope, hair follicle units were manually count, the results are shown in Table 6. The mice received plant extracts showed higher hair follicles than that received vehicle and minoxidil. There was no significant difference in hair follicle number between the mice that received minoxidil

and vehicle. All of three plant extracts promoted hair follicle proliferation in mice better than vehicle ($p < 0.05$) and safflower extract promoted hair follicle proliferation in mice better than minoxidil ($p < 0.05$).

Table 6 Effects of vehicle, minoxidil, safflower, butterfly pea and emblica extract on hair follicle count in C57BL/6 mice.

Tested compound	Mean hair follicle count ¹
Vehicle (ethanol:propylene glycol:water)	24.2 ± 2.8
Minoxidil	36.3 ± 4.1
Safflower extract	69.5 ± 7.6*
Butterfly pea extract	52.5 ± 6.1*
Emblica extract	46.4 ± 3.0*

* indicated significantly differences from vehicle ($p < 0.05$)

¹ values in Table expressed as mean ± SD of five C57BL/6 mice

From these results, there was a strong relationship between FEA value and hair growth promoting activity of the extract (as hair growth score) ($r = 0.719$) in day 14 of the treatment period. There also was a strong relationship between FEA value and hair follicle number ($r = 0.766$).

All of the results suggested that safflower is the most potent hair growth promoter in mice, which its mechanism of action may occur from 5α -reductase inhibition and hair follicle proliferation promotion. From this point, safflower extract will be developed into the topical product to treat hair loss in the following parts.

4. Formulation and assessments of NLC bases

As previously discovered by the researchers that only substances size less than 1000 nm are able to absorb into the hair follicles (Schaefer and Lademann, 2001), the special carriers was crucially needed. The lipid nanoparticles (LN) have been developed in the beginning of the 1990s, for substitution the traditional emulsions, liposomes and other carriers (Lucks and Müller, 1996). LN provides many benefits than traditional carriers, but the important characteristics are the protection of entrapped substance from environmental degradation and the prolonged-release property (Mehnert and Mäder, 2001, Wissing and Müller, 2003). Since there are two generations of the LN, the SLN and the NLC, the NLC provides more benefits than SLN in an entrapment of substances (Müller et al., 2002). In this study NLC was developed as the suitable and stable carrier for delivery the safflower extract into hair follicle and exerts the 5α -reductase and hair growth promoting activity. Before an entrapment of safflower extract into the NLC, the appropriate base was needed. From references, the main formula or F1 was modified from Han et al. (2008). The modified compositions of trial formulations are listed in the Table 7.

The reference formula (Han et al., 2008) used monostearin as a wax matrix with an incorporation of medium chain triglyceride (MCT) with the wax:oil ratio of 6:4. Incorporation of MCT or other liquid lipid material make the NLC more capable to load substances since the liquid lipid material impaired the crystallinity of the wax matrix, therefore decreased the drug expulsion from NLC. In addition, increasing of the liquid lipid content did not affect the particle size of the NLC, but affected the zeta potential of the NLC (Teernachaideekul et al., 2008).

Table 7 Formulation of NLC

Ingredients		% (w/w)								
		F1	F2	F3	F4	F5	F6	F7	F8	F9
A:	Monostearin	7	7	7	7	7	7	7	7	7
	Medium chain triglycerides	3	3	3	3	3	3	3	3	3
	Brij-L4 (Laureth-4)	-	1	-	1.43	1.45	1.4	0.5	1	1
	Span 60	-	-	-	-	5.7	-	9.5	9.5	9.5
	Span 80	-	-	5.5	5.63	-	-	-	-	-
	Span 83	-	-	-	-	-	5.52	-	-	-
	Tween 80	2	2	-	-	-	-	-	-	-
	Tween 60	-	-	-	-	-	-	-	2	2
	Pluronic F-68	2	2	2	2	2	2	2	2	2
	Sodium deoxycholate	0.5	0.5	0.8	0.6	0.6	0.59	0.5	-	-
B:	Sodium cocoylisethionate	-	-	-	-	-	-	-	-	0.7
	DMDM hydantoin	-	0.2	0.2	0.2	0.2	0.2	0.2	0.2	0.2
	DI water	85.5	84.3	81.21	79.8	79.81	79.8	78.8	75.3	74.6

However, increasing amount of the liquid lipid can cause supercooled melts; which is the state that the waxes matrix of the NLC occurred as a liquid at room temperature where the temperature is lower than their melting point (Teernachaideekul et al., 2008). The wax:oil ratio of F1 formula was modified from the references of Han et al. (2008) to 7:3. After preparation, F1 formula showed the crystal growth at the bottom of the container after prepared for 48 h. The mold growth was observed in F1 after prepared for 7 days. From described problem, this formula needed to be improved into F2 by addition of Brij-L4 and DMDM hydantoin. Brij-L4 was added in order to aid in the solubilization of safflower extract in the next part of this study. DMDM hydantoin is a preservative. After prepared for 3 days, this F2 formula had a crystal growth and became gelation.

F3, F4, F5 and F6 formula were developed from F2 by changing the emulsifiers. The amount of the emulsifiers needed to use was calculated from a hydrophilic-lipophilic balance (HLB) profile of the oil phase (Required HLB of an oil phase was 6.19). However the instability was also occurred in all of these formulae. Suggesting that only calculation of HLB alone may not be adequate in a stabilization of the NLC.

In F7 formula, higher amount of span 60 had used to provide more stability, and this was a successes move since the stability of the formulation increased to a few months. Span 60 is a nonionic surfactant, which may act as a steric hindrance at the particle surface to prevent agglomeration of the particle (Mithri et al., 2011). However, the F7 formula provided only short term stability. Therefore, the anionic surfactant sodium deoxycholate was replaced with sodium cocoyl isethionate (SCI).

In order to compare the effect of SCI on stability of NLC, F8 and F9 formulae were developed. F8 was used as a control for F9. From data of F8 and F9, addition of SCI did improve the stability and physical appearance of the NLC.

Heating-cooling cycles were used as a screening stability test for determination of long-term stability. F9 had passed this accelerated stability test, with no changes in physical appearances, particle size and size distribution.

The averages particle size, size distribution at 1 day after preparation and physical stability of all formulae are listed in Table 8. The results suggested that NLC with SCI provided more stability profile than in the NLC without anionic surfactant and sodium deoxycholate. The usage of DMDM hydantoin as a preservative in the formulations was effective, since there were no microbial spoilages on the products even being kept at the room temperature over than 1 year.

Table 8 Average particle size at day 1 and stability of formulated NLC

Formula	Average particle size (nm)	Polydispersity index	Stability
F1	120.1 ± 0.5	0.341 ± 0.014	2 days (Crystal growth)
F2	75.3 ± 0.9	0.322 ± 0.041	3 days (Gel)
F3	127.2 ± 3.9	0.263 ± 0.037	7 days (Crystal growth)
F4	106.2 ± 4.9	0.231 ± 0.032	14 days (Crystal growth)
F5	125.0 ± 3.4	0.234 ± 0.017	7 days (Crystal growth)
F6	114.6 ± 1.8	0.214 ± 0.012	1 months (Gel)
F7	128.5 ± 3.6	0.197 ± 0.012	3 months (Crystal growth)
F8	169.7 ± 3.8	0.275 ± 0.014	1 months (Gel)
F9	106.6 ± 1.1	0.216 ± 0.005	More than 1 year

Since F9 was the most stable formula, it will be used in further experiments. Morphology of the F9 was assessed by TEM, the result is presented in Figure 16. TEM micrograph suggested that the particle of F9 occurred as a spherical in shape with approximate diameter of 200 nm.

The physical parameters of lipid crystallinity and long term stability of F9 were studied. Lipid crystallinity of F9 was firstly checked by DSC and the thermogram is shown in Figure 17.



Figure 16 TEM image of F9 NLC particle, one bar length indicated 200 nm

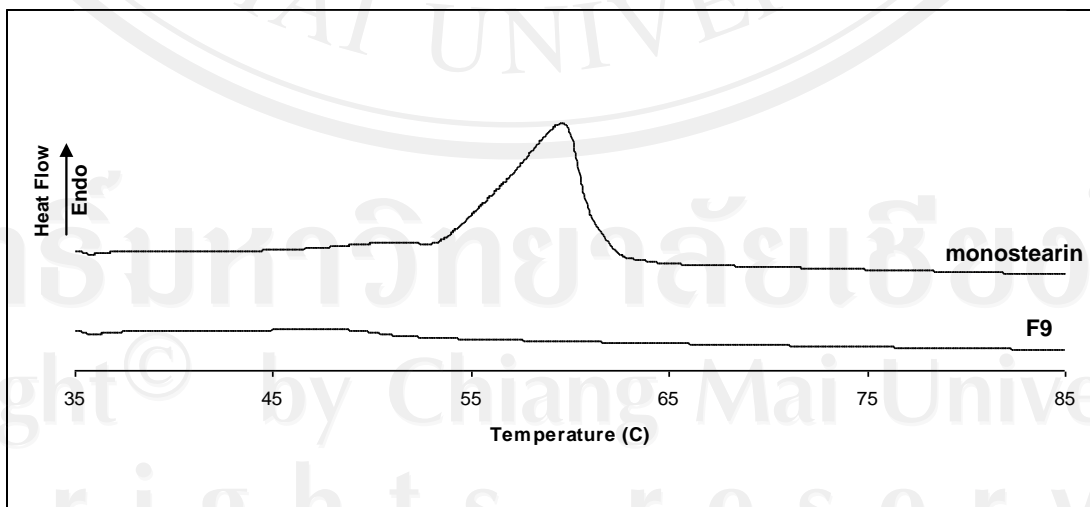


Figure 17 DSC thermogram of pure monostearin and F9

The data obtained from DSC usually provides the melting point and crystallization behavior of the lipid nanoparticles (Lin et al., 2007). From DSC results, monostearin gave the onset of melting at 54.346 °C, melting point was 59.593 °C and the enthalpy (ΔH) was 121.608 J/g. Normally, these parameters help us calculated the lipid crystallinity of the lipid nanoparticles. The higher lipid crystallinity, the lower entrapment efficacy is. In the NLC F9, none of the onset of melting and the melting peak was observed. Usually, the disappearance of the melting phenomena of the lipid nanoparticles are from three causes; i) the homogenously dispersed of the loading chemical in the wax matrix ii) the wax matrix is occurred as the supercooled melts or iii) the wax matrix is amorphous state. For further confirmation, the XRD or raman spectroscopy is needed (Jores et al., 2005, Mithri et al., 2011).

In order to confirm the results obtained from DSC, XRD was used and the X-ray diffraction pattern of pure monostearin and F9 are shown in Figure 18.

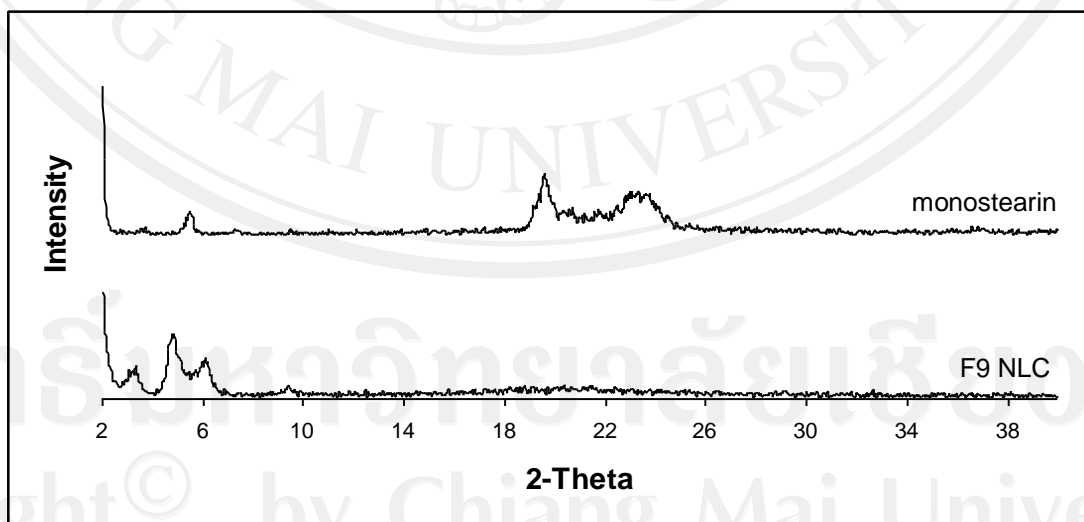


Figure 18 X-ray diffraction pattern of pure monostearin and F9

The data obtained from X-ray diffraction provided the inner structure of the lipid nanoparticles and the changes of the microstructure in the lipid crystallization process (Lin et al., 2007). From Figure 18, the diffractogram of monostearin exhibited sharp peak at $2\theta = 19.6^\circ$ and broad peak between $2\theta = 22.2^\circ$ to 25.0° . Compare to the NLC F9 the disappearance of the signature peaks found in monostearin was observed, suggesting that the NLC F9 was amorphous, which was in the same direction of that obtained from DSC. Usually, incorporation of liquid lipid into the wax matrix of lipid nanoparticles does not change the signal position but depresses the signal intensity (Lin et al., 2007). However, the disappearance of the signal in this case suggested that the core has no crystalline structure. Amorphous wax matrix provides more benefits in the entrapment of active substance, which lipid recrystallization was not occurred. So the drug expulsion processes will not occur in this type of NLC.

Long term stability of F9 was studied by keeping at room temperature for 1 year. There were no change in physical parameters of physical appearance, particle size, size distribution and zeta potential. The comparison of size distribution of the F9 in the different time after keeping is shown in Figure 19.

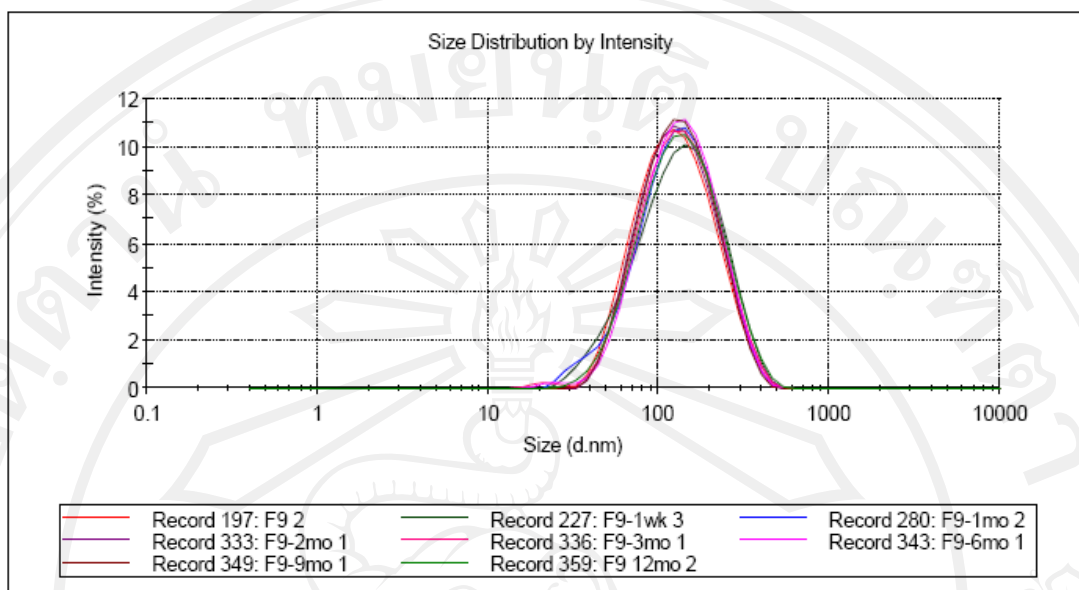


Figure 19 Comparison of the particle size distribution of F9 in one year after being kept at room temperature

Figure 19 is the cumulative plots of the intensity of particle (in percentage) by size (in nm). The unchange in size distribution curve and polydispersity index between day 1 and 1 year along with the unchange in the size distribution curve suggested that the NLC F9 was stable at least 1 year after preparation. From the results, the NLC F9 will be used in an incorporation of safflower extract in the next part of the study.

5. Formulation and assessments of safflower extract-loaded NLC (CT-NLC)

From the previous part of the study, safflower extract was the most potent 5α -reductase inhibitor and hair growth promoter. Normally, the safflower extract is water soluble, but the use of Brij-L4 has helped safflower extract to be soluble in oil.

Formulation of an entrapped safflower was shown in the Table 9. Five concentration of safflower extract, which were 0.05, 0.1, 0.25, 0.5 and 1 % by weight were studied. The codes F9L1, F9L2, F9L3, F9L4, and F9L5 were given to these preparations.

Table 9 Formulation of safflower-entrapped NLC

Ingredients	% (w/w)				
	F9L1	F9L2	F9L3	F9L4	F9L5
Safflower extract	0.05	0.1	0.25	0.5	1
Monostearin	7	7	7	7	7
Span 60	9.5	9.5	9.5	9.5	9.5
Medium chain triglycerides	3	3	3	3	3
Brij-L4	1	1	1	1	1
Pluronic F-68	2	2	2	2	2
Tween 60	2	2	2	2	2
Sodium Cocoylisethionate	0.7	0.7	0.7	0.7	0.7
DMDM hydantoin	0.2	0.2	0.2	0.2	0.2
DI water	74.55	75.5	74.35	74.1	73.6

The higher of concentration of safflower extract used in the system, the higher viscosity of formulation was observed. In the formula with the highest concentration of safflower (F9L5); 1 % by weight of safflower extract, occurred as a high viscosity macroemulsion. Therefore, F9L5 was excluded from the study.

Particle size, size distribution and zeta potential of these safflower-entrapped formulations are shown in Table 10.

Table 10 Particle size, size distribution and zeta potential of safflower-entrapped formulations compared with unentrapped NLC or F9

Formula	Average particle size (nm)	Polydispersity index	Zeta potential (mV)
F9	106.6 ± 1.1	0.216 ± 0.005	-42.0 ± 0.5
F9L1	108.7 ± 1.9	0.222 ± 0.009	-49.2 ± 2.9
F9L2	109.2 ± 0.8	0.214 ± 0.006	-41.8 ± 2.2
F9L3	104.0 ± 1.3	0.195 ± 0.008	-40.4 ± 2.2
F9L4	111.5 ± 0.3	0.194 ± 0.007	-44.3 ± 0.2

From Table 10, the particle size, size distribution and zeta potential of entrapped formulation were not difference from the unentrapped F9 NLC, suggesting that incorporation of the safflower extract into the wax matrix was not interfere to the NLC system. Other than real time room temperature kept for stability study, the heating cooling cycles was also used. All entrapped formula passed this stressed stability test. In addition, entrapped formulas provided more than 1 year stability when kept at room temperature. The size distribution of all formulated products after keeping for 1 year were shown in the Figure 20, 21, 22 and 23, respectively

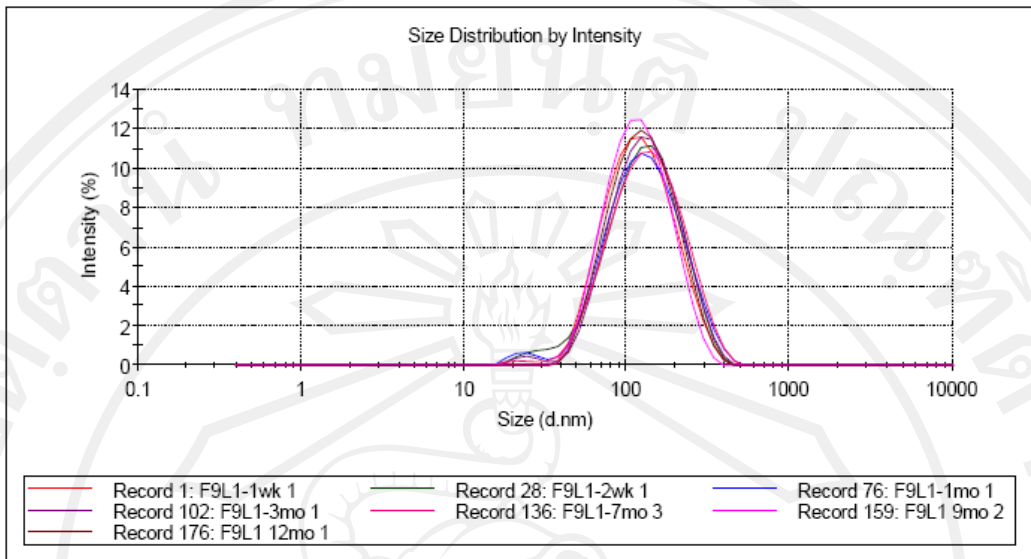


Figure 20 Comparison of the particle size distribution of F9L1 in one year after being kept at room temperature

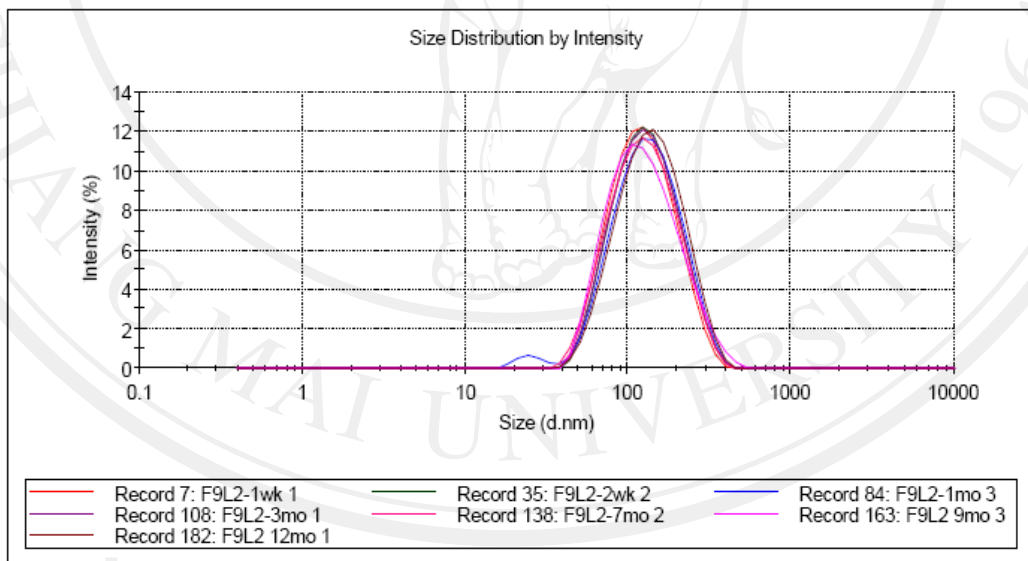


Figure 21 Comparison of the particle size distribution of F9L2 in one year after being kept at room temperature

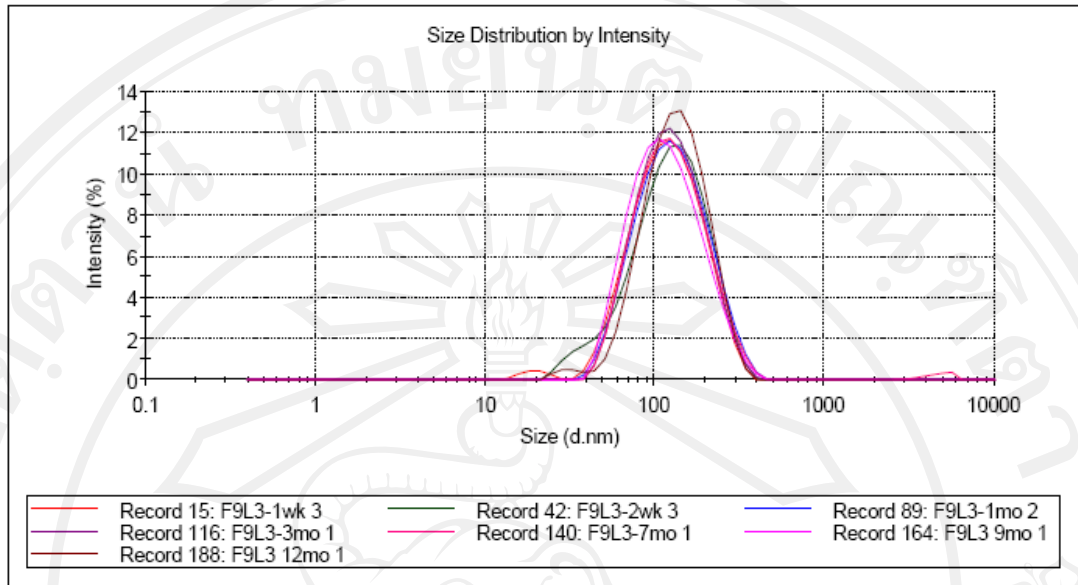


Figure 22 Comparison of the particle size distribution of F9L3 in one year after being kept at room temperature

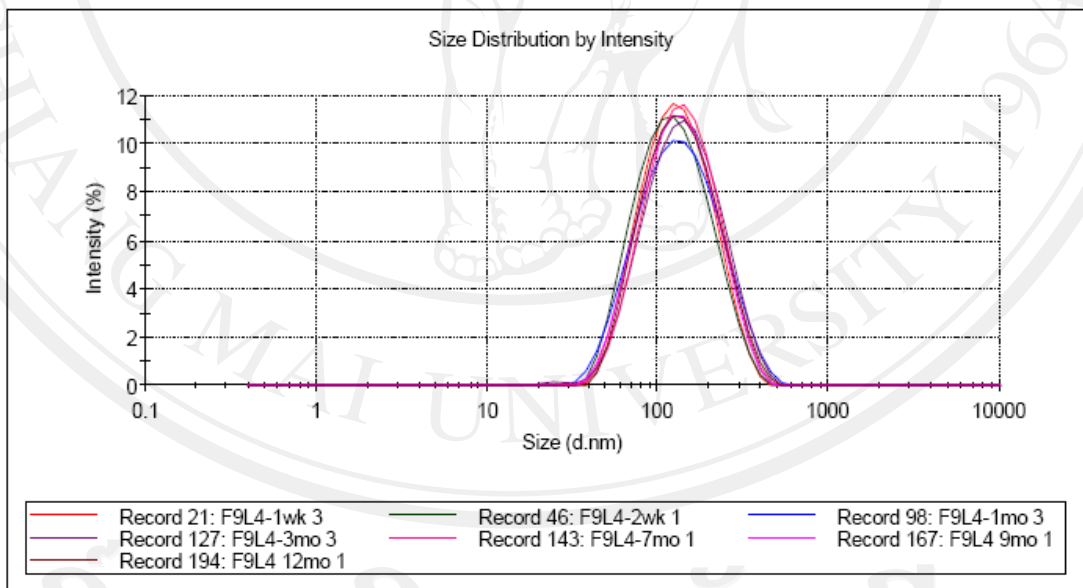


Figure 23 Comparison of the particle size distribution of F9L4 in one year after being kept at room temperature

Comparison of the size distribution curves of these particles suggested that stable particle was achieved when using SCI as an anionic surfactant.

Previously published research articles indicated that zeta potential greater than absolute of 30 provide good stability to lipid nanoparticles (Mehnert and Mäder, 2001, Mithri et al., 2011). Thus, this can explain the physical stability of all CT-NLCs.

TEM micrographs of all entrapped formulae occurred in the same pattern. The TEM micrograph of F9L2 is represented in the Figure 24.

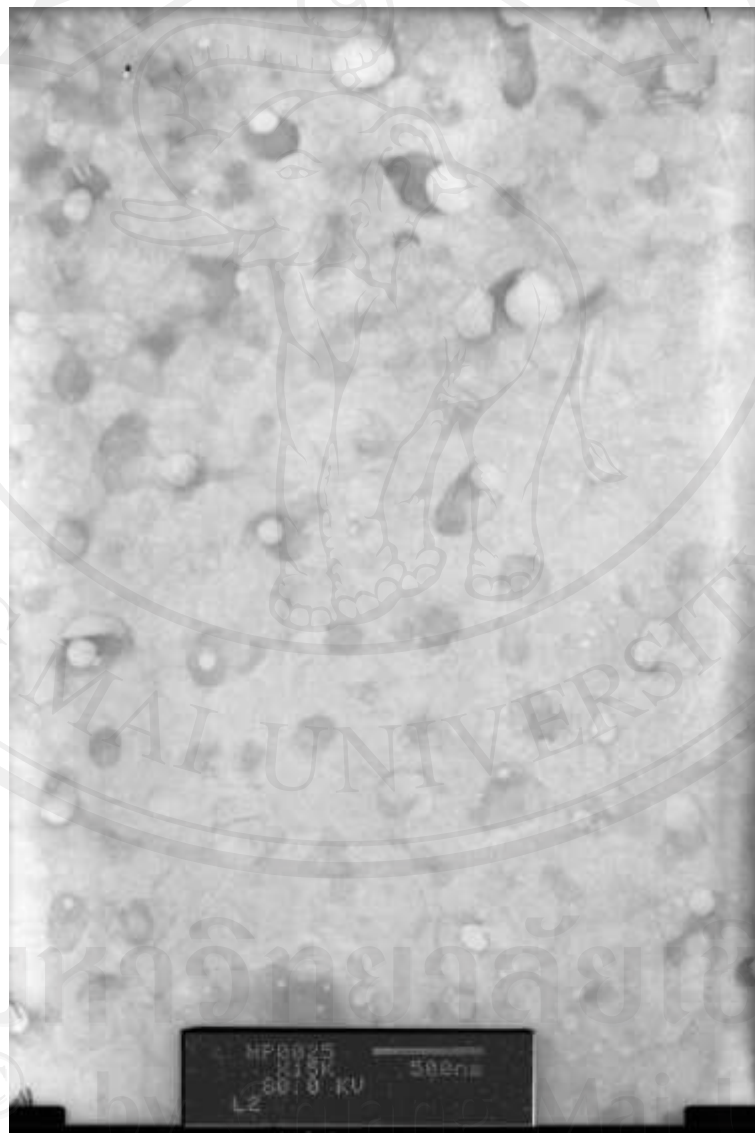


Figure 24 TEM micrograph of F9L2, one bar length indicates 500 nm

From Figure 24, average particle size of F9L2 was nearly 100 to 200 nm, which was correlated with the results from PCS technique.

In order to determine the entrapment efficacy, the suitable analytical procedure is needed. Cold methanol precipitation technique was used to extract untrapped safflower from NLC system. Extracted components were screened for the UV absorbance over the region of 200 to 500 nm, versus the standard safflower yellow and safflower extract. The results revealed that the most suitable wavelength for determination of safflower yellow in extracted NLC was 401 nm (Figure 25).

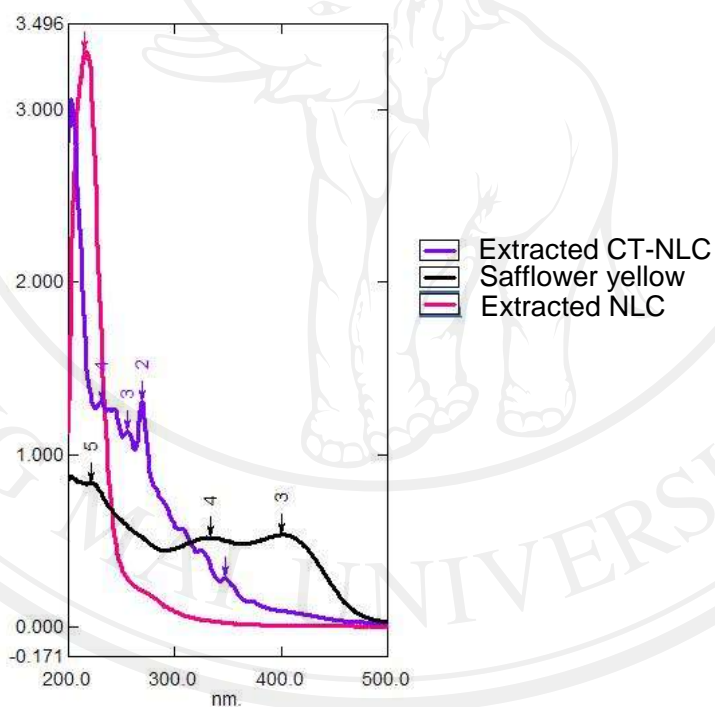


Figure 25 UV absorbance spectrums screening of extracted CT-NLC, safflower yellow and extracted NLC, showing the suitable wavelength for determination of safflower yellow at 401 nm.

Although there are many previous published methods for determination of substances in safflower extract, those techniques required complex procedures such as

HPLC/DAD/ESI-MS (Jin et al., 2008) and HPLC/MS-MS (Wen et al., 2008) methods. Some published method takes a long time of analysis. For example, the HPLC/DAD method developed by Fan et al. (2009) was the gradient HPLC condition that took over 70 minutes per one analysis. From these reasons, the simple isocratic HPLC-UV method for determination of safflower yellow in the extracted sample was developed and validated. From given HPLC condition, the analysis time per one sample was as shorter as 10 min, if include the lag time for cleaning the injector's needle and re-equilibrating the system was not exceed 20 min per analysis. With this isocratic condition, the standard safflower yellow gave retention time at around 2.5 min. HPLC chromatogram of standard safflower yellow is shown in Figure 26.

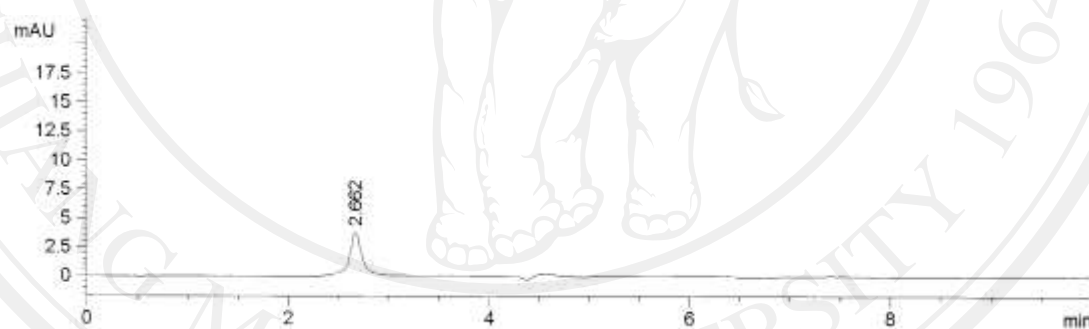
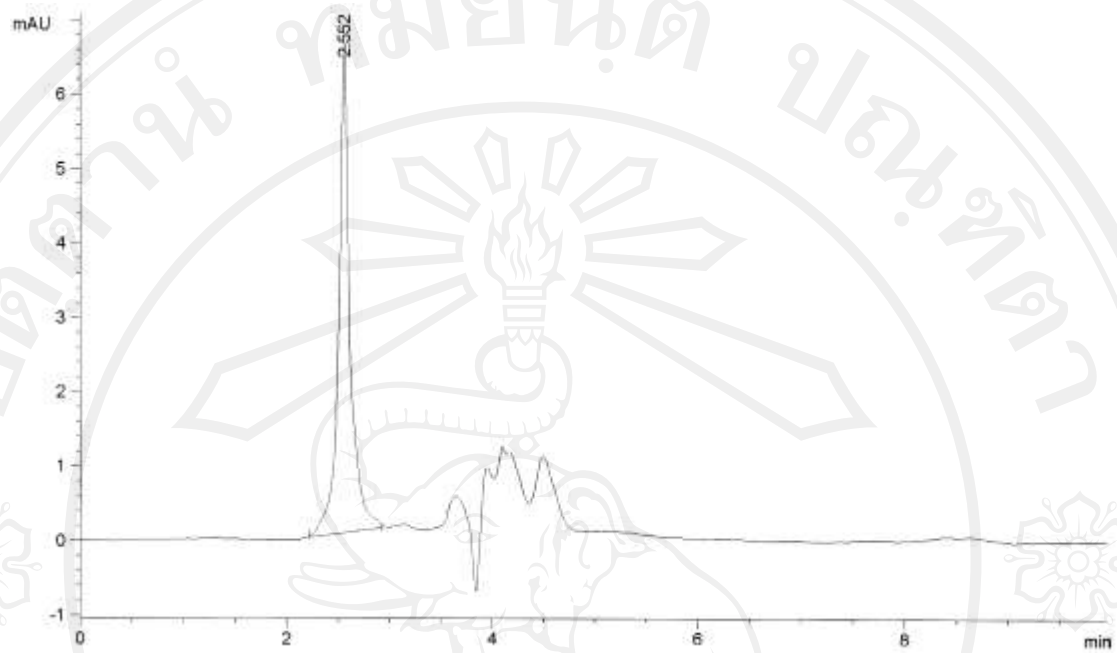


Figure 26 HPLC chromatogram of standard safflower yellow

The safflower extract was also analyzed by this method, its chromatogram is shown in Figure 27A. For confirmation of the retention time, standard safflower yellow was spiked into the safflower extract; the chromatogram of spiked safflower extract is shown in Figure 27B.

A:



B:

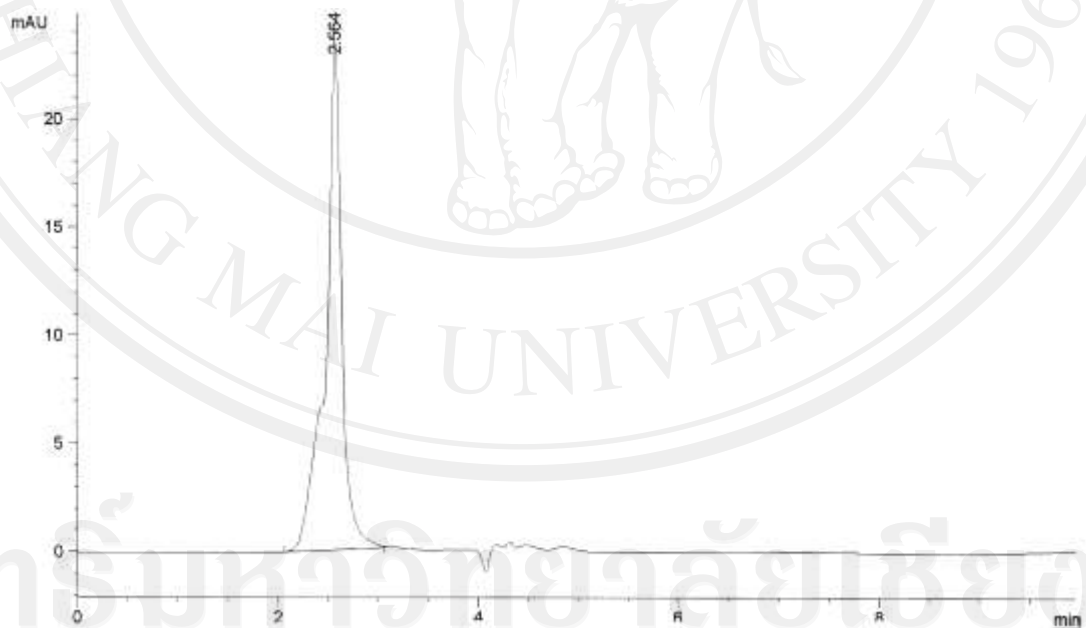


Figure 27 HPLC chromatogram of (A) safflower extracted and (B) safflower yellow spiked safflower extract, the safflower yellow showed intensified peak at 2.5 min (note: different scale of figure 27A and 27B)

After addition of the standard safflower yellow, the intensity of the peak at 2.5 min was shown a remark increased, suggested that the intensity of this peak was really caused from the concentration of the safflower yellow.

The chromatogram of extracted CT-NLC and spiked CT-NLC are shown in Figure 28A and B, respectively.

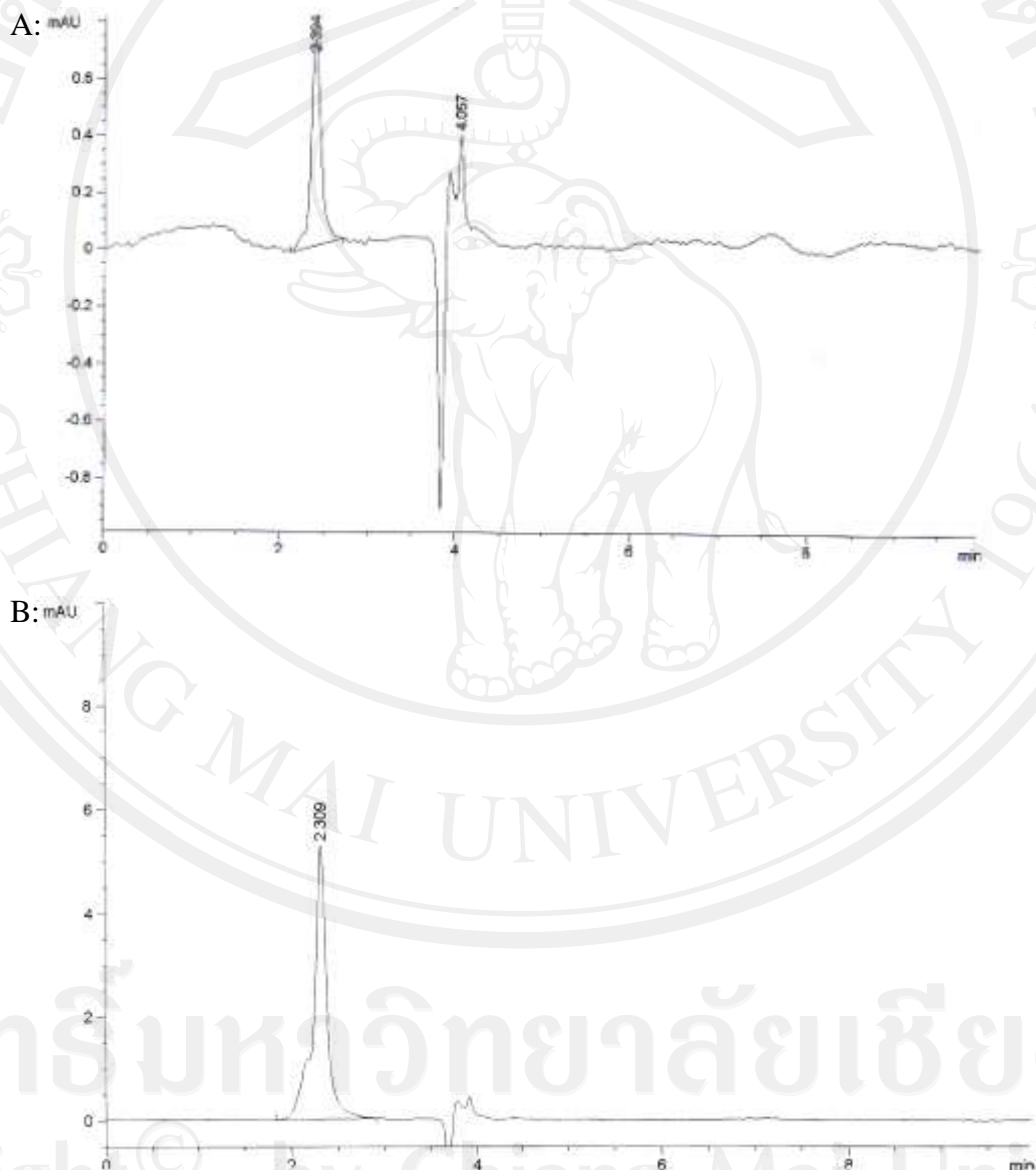


Figure 28 HPLC chromatogram of (A) extracted CT-NLC and (B) safflower yellow spiked CT-NLC (note: different scale of figure 26A and 26B)

For validation of the conducted method, the validation parameters under the ICH were used.

Accuracy and precision of this conducted method is shown in Table 11.

Table 11 Accuracy and precision of HPLC-UV method for determination of safflower yellow in NLC

Concentration (ppm)	% recovery	RSD (%)	
		Repeatability	Intermediate precision
5	101.41 ± 0.93	1.78	2.12
10	101.14 ± 4.96	6.48	5.49
25	95.98 ± 4.45	5.17	4.62
50	100.40 ± 1.74	1.82	3.08
75	102.57 ± 4.03	4.06	3.57
100	98.68 ± 3.46	3.60	6.21

From Table 11, % recovery and RSD were not regarded to the concentration of safflower yellow. % recovery of the method was in the range of 95.98 to 102.57%, which is conformed to the USP/NF, that usually accepted the range between 95 to 105%. RSD of the method was in the range of 1.78 to 6.48%. From Horwitz equation (Horwitz et al., 1980), which is the equation used for estimated the acceptable RSD from different concentration level of the analyte, reproducibility standard deviation (RSD_R) of analyte at contraction from 5, 10, 25, 50, 75 and 100 ppm were 12.56, 11.31, 9.86, 8.88, 8.35, and 8 %, respectively. The data from Table 11 suggested that RSD from this method are conformed to Horwitz equation.

Specificity of conducted method was validated by peak purity of the main peak at retention time around 2.5 min by UV spectrum scanning and mass spectrum scanning. UV spectrum scanning of main peak at retention time around 2.5 min of standard safflower yellow, safflower extract, and extracted CT-NLC, are shown in Figure 29A, B and C, respectively.

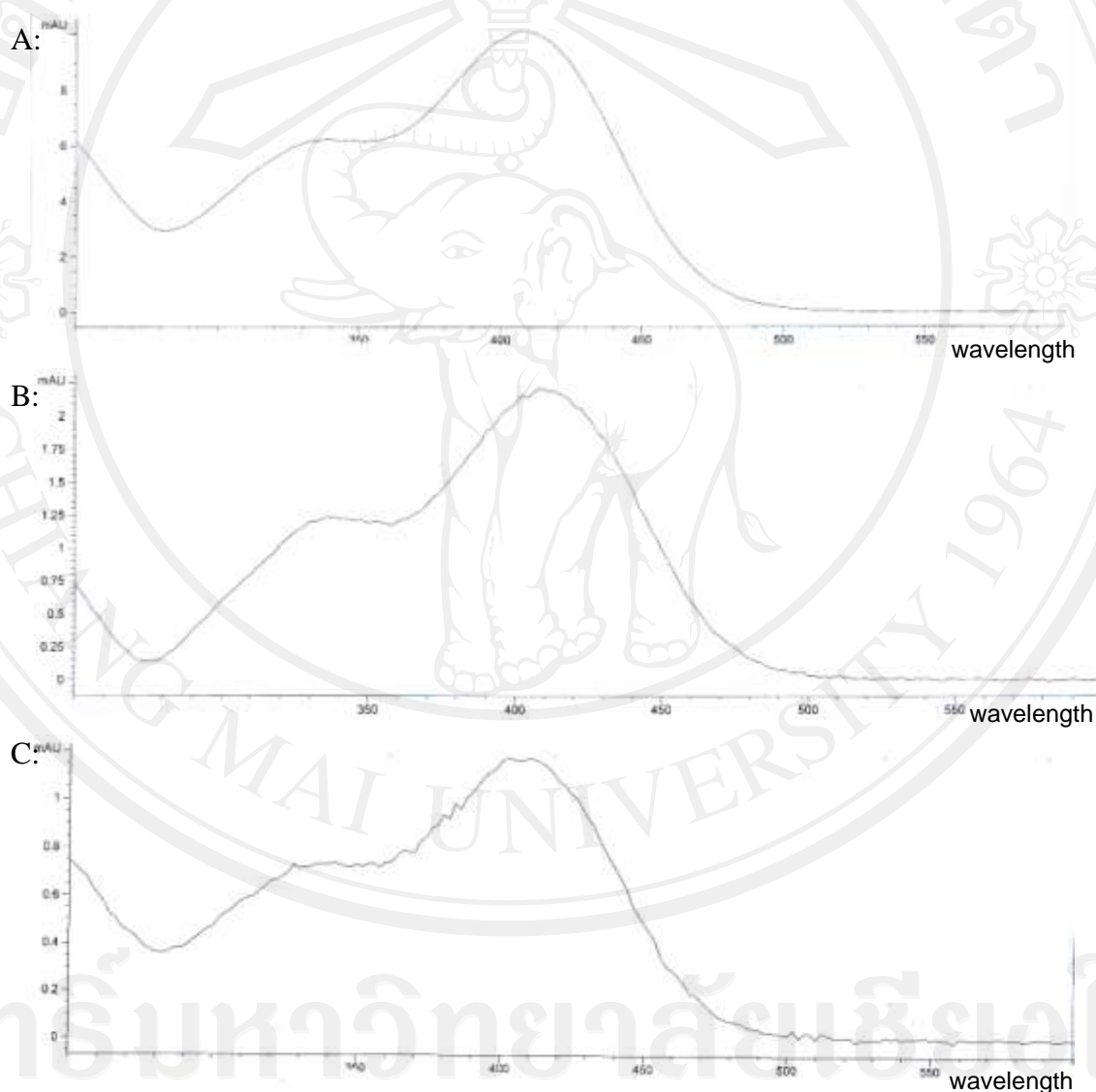


Figure 29 UV spectrum scanning of (A) standard safflower yellow (B) safflower extract and (C) extracted CT-NLC

Mass spectrum scanning of main peak at retention time around 2.5 min of standard safflower yellow, safflower extract, and extracted CT-NLC, are shown in Figure 30A, B and C, respectively.

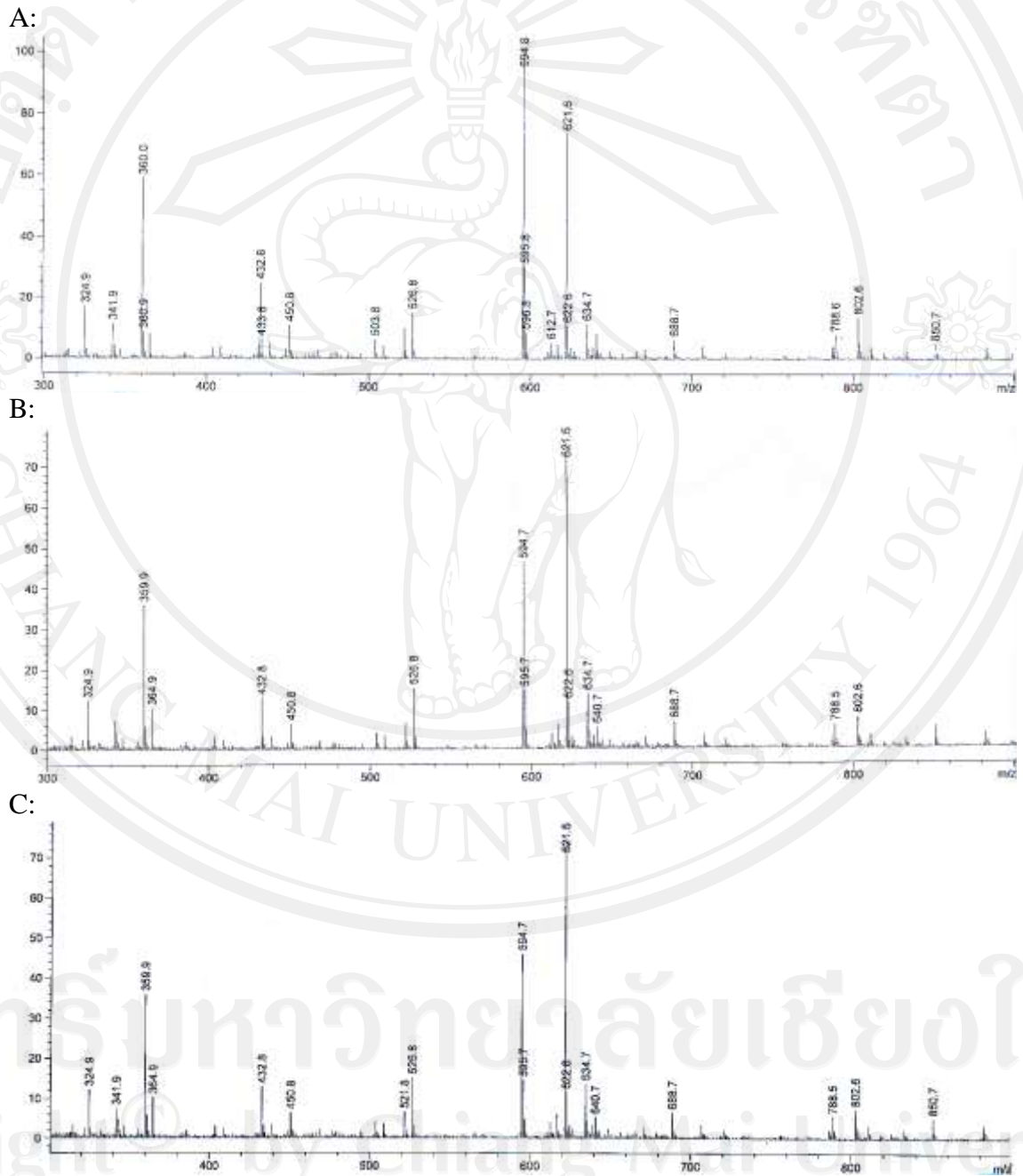


Figure 30 HPLC/ESI mass spectrum scanning of (A) standard safflower yellow (B) safflower extract and (C) extracted CT-NLC

From Figure 29 and 30, the UV spectrum and mass fragment pattern from peaks of different analytes suggested that this method provided specificity in an analysis for safflower yellow. Comparison of dominant mass peak of all analyzed sample from Figure 29 are shown in Table 12.

Table 12 The result of HPLC/ESI-MS screening and characterization of safflower yellow, safflower extract, and extracted *Carthamus tinctorius* L.-loaded Nanostructured lipid carriers (CT-NLC).

Test compound	Dominant HPLC/ESI-MS <i>m/z</i>
Safflower yellow	594.8, 621.6, 360.0, 432.8, 526.8, 634.7
Safflower extract	621.6, 594.7, 359.9, 526.8, 432.8, 634.7
Extracted CT-NLC	621.6, 594.7, 359.9, 526.8, 432.8, 634.7

Twelve concentrations of safflower yellow over the range of 5 to 250 ppm were analyzed by this conducted method. Linearity range was found in the concentration range of 5 to 100 ppm. The standard curve of safflower yellow is shown in Figure 31.

LOD, which is the lowest concentration of safflower yellow that this method can be detected, and LOQ, which is the lowest concentration of safflower yellow of that this method can be accurately and precisely quantitized, were assessed. LOD and LOQ of this method were 1.4 and 4.1 ppm, respectively.

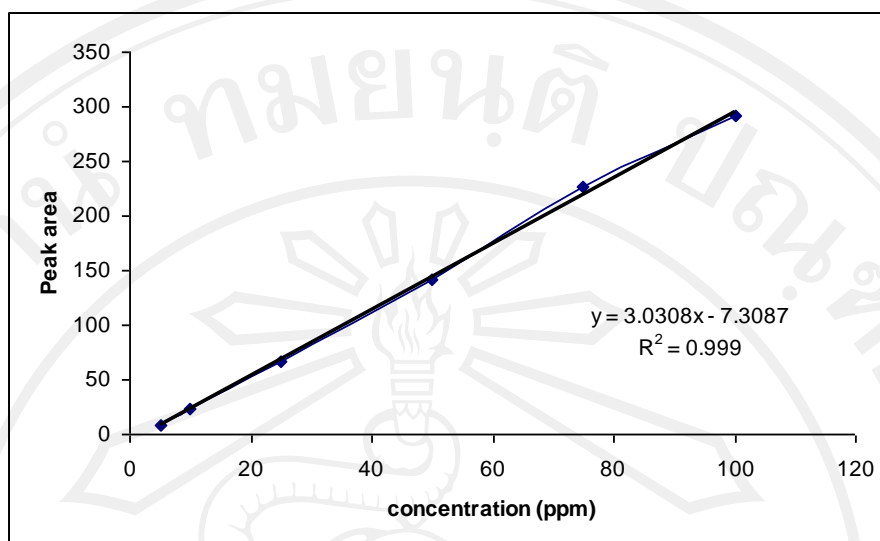


Figure 31 Standard curve of safflower yellow

Entrapment efficacy (EE) of safflower extract into the wax matrix of NLC was calculated by indirect method, which detecting the unentrapped safflower extract in the matrix. Usually the EE analysis substances in lipid nanoparticles are mostly done by indirect method. For example, Teeranachaidekul et al. (2007) assessed the EE of Q₁₀ in the NLC by using ultrafiltration method. Hu et al. (2006) also assessed the EE of clobetasol propionate in monostein NLC by using indirect method. The NLCs were freeze-drying prior to the analysis by dispersing the NLC powder in surfactant solution. In this study, cold methanol was used as a wax precipitation enhancer due to three hypotheses; i) most of the substances have less solubility when the temperature is lower ii) solubility of waxy material in methanol is very low and iii) methanol can caused dehydration effect, which hydrodynamic stabilized layer between the lipid nanoparticles are destroyed after addition of methanol. From three explained reasons, the wax matrix of the NLCs are agglomerated and crystallized, where the solubilized safflower extract in medium or vehicle of NLC are extracted in the methanol phase.

From the condition used, there was a mild condition that the wax could not be ruptured or released the substances from the wax core where the entrapped safflower extract is well-protected. From the characteristics of NLC that is a solidified core, the entrapped substances could not be exchanged to the environment (Wissing and Müller, 2003). For confirmation of this hypothesis the direct method was also used. The UV spectrum scanning of the wax matrix after crystallized by the methanol precipitation was done and the HPLC analysis was also conducted.

UV spectrum scanning of dissolved wax matrix after crystallization by methanol precipitation technique is shown in Figure 32. The F9 NLC was used as a control.

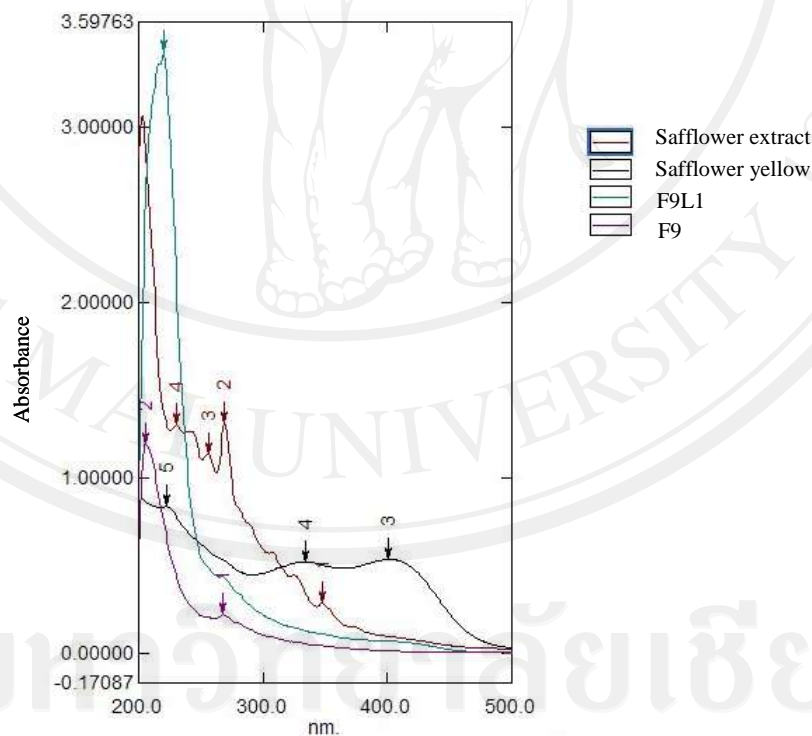


Figure 32 UV spectrum of the wax matrix of F9 and F9L1, comparing with safflower extract and safflower yellow

From Figure 32, there is an absorbance of substance in the spectrum of F9L1. This suggested that the safflower extract was well-protected in the wax core, and the wax was not released the safflower extract during the cold methanol precipitation process. The further confirmation was conducted by HPLC analysis. HPLC chromatogram of dissolved wax matrix of F9L1 is shown in Figure 33.

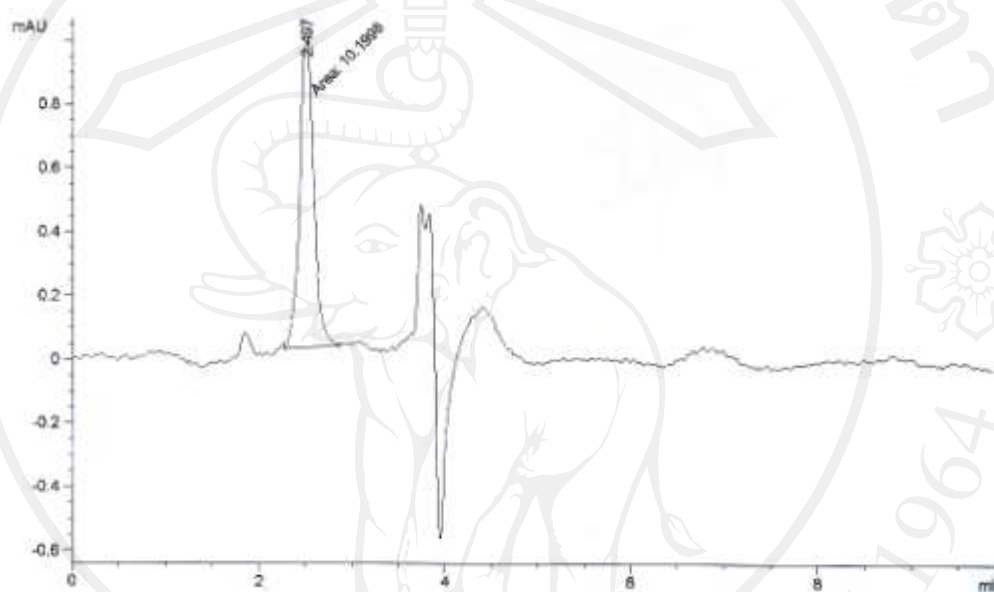


Figure 33 HPLC chromatogram of dissolved wax matrix of F9L1, the safflower yellow showed intensified peak at 2.5 min.

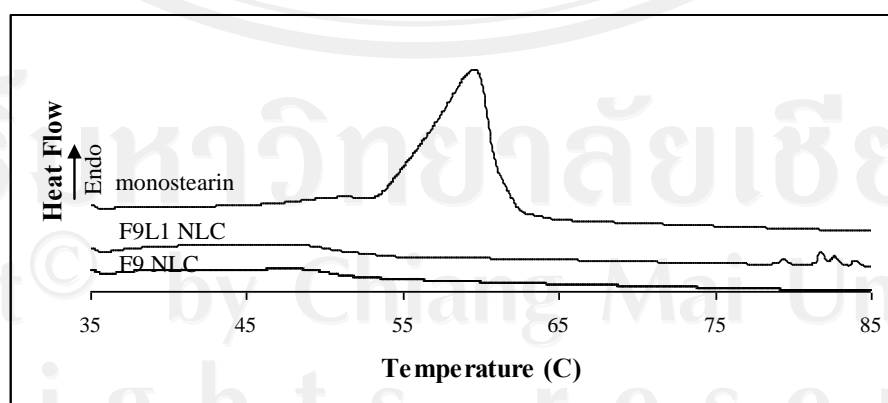
From Figure 33, there is the peak of safflower yellow at retention time of 2.5 min. This suggested that the indirect method used in determination of EE was appropriate. The direct method was not preferable than that indirect one because of frustration and losses of the substance in an extraction process.

The EE and loading capacity of safflower extract into NLCs from monostearin are shown in Table 13.

Table 13 Entrapment efficacy and loading capacity of safflower extract

Formula	Concentration of loaded safflower extract (% w/w)	Entrapment efficacy (%)	Loading capacity (%)
F9L1	0.05	76.3 ± 5.5	0.04 ± 0.01
F9L2	0.1	67.6 ± 3.1	0.07 ± 0.02
F9L3	0.25	55.9 ± 2.2	0.14 ± 0.02
F9L4	0.5	52.0 ± 1.8	0.26 ± 0.06

From Table 13, Concentration of safflower extract loaded in the NLC affected the EE of the NLC. The higher concentration used, the lower EE was. However, the results were contrasting to the loading capacity since the loading capacities increased after increasing the concentration of safflower extract. This was contradict to the previous work of Hut e al. (2006), which EE and loading capacity was proportionally related in the same direction. The results suggested that F9L1, with 0.05 % by weight of safflower, shown the highest EE. The crystallinity of F9L1 was firstly checked by using DSC and then confirmed by XRD, the results are shown in Figure 34 and 35, respectively.

**Figure 34** DSC thermogram of F9L1, comparing with F9 and monostearin

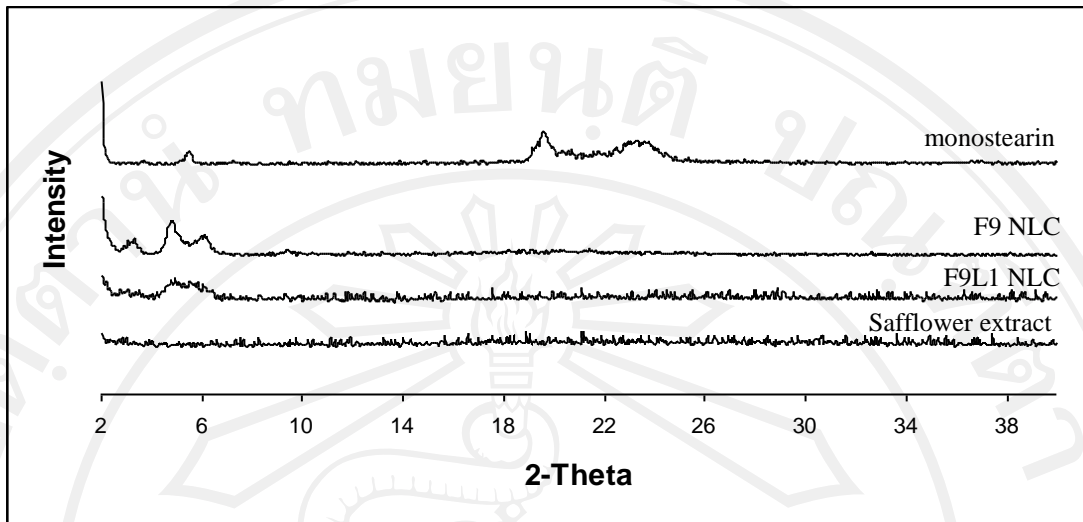


Figure 35 X-ray diffraction pattern of F9L1, comparing with monostearin, F9, and safflower extract

From DSC thermogram (Figure 34), F9L1 did not show any thermal event as same as the F9 NLC. The result from XRD has confirmed that the F9L1 was also occurred as the amorphous type NLC.

Chemical stability of entrapped safflower extract in F9L1 after prepared for 1 year is shown in Table 14

Table 14 Chemical stability of entrapped safflower extract in F9L1

Duration after preparation	Percentage of entrapped safflower extract
1 Day	100.0
6 Months	96.7 ± 2.1
1 Year	97.2 ± 1.8

From Table 14, there was no significant difference in safflower extract content in the wax matrix. This suggested that F9L1 NLC could protect the safflower extract

from environmental degradation. From these results, F9L1 was selected as the most appropriate formula to be further developed into the hair lotion.

6. Formulation and assessment of hair lotion containing NLC

The results from previous part of the study suggested that F9L1 was the most appropriate formulation. F9L1 was used in the formulation of nano-hair lotion, because of its better physicochemical profile. Three different dosage forms, which were hydrogel, nanosuspension and o/w emulsion were studied.

The hydrogel formula composed of:

Rx	% w/w
Carbopol 940	0.1
F9L1	5
DMDM hydantoin	0.1
DI water	94.8

The nanosuspension formula composed of:

Rx	% w/w
F9L1	5
DMDM hydantoin	0.1
DI water	94.9

The o/w emulsion formula composed of:

Rx	% w/w
A: Chremophore A-6	3
Chremophore A-25	1
Stearic acid	3
Glyceryl monostearate	4
BHT	0.1
B: Propylene glycol	5
EDTA	0.1
Triethanolamine	1.4
DMDM hydantoin	0.1
Metyl paraben	0.1
Propyl paraben	0.02
DI water	77.18
C: F9L1	5

After preparation, the hydrogel formula stimulated the agglomeration of wax particle of NLC. The emulsion appeared as a milky easily dispersed liquid. The nanosuspension appeared as a translucent liquid.

Other than heating-cooling cycle, the stability of the nanosuspension and o/w emulsion was also tested under the criteria from Thai Industrial Standard No. 152-2539, using centrifugation at 6000 rpm for 30 min. No change in physical appearance of the formulation was observed; this suggested the stability of these formulations.

Particle size of these three dosage forms were also investigated, the results are shown in Table 15.

Table 15 Particle size of hydrogel, nanosuspension, and o/w emulsion containing safflower-entrapped NLC

Dosage form	Average particle size (nm)	Poly dispersity index
Hydrogel	120.1 ± 1.3	0.199 ± 0.010
Nanosuspension	110.4 ± 0.7	0.206 ± 0.014
o/w emulsion	292.2 ± 4.5	0.612 ± 0.083

From Table 15, both hydrogel and nanosuspension showed appropriate size and size distribution, but stability of hydrogel was not good since the wax matrix of NLC in hydrogel was agglomerated. In the o/w emulsion, the PCS technique may not be suitable for analysis of particle size and size distribution since there are two different particles from oil droplet and the NLC dispersed in the same medium, which can explain from size distribution curve in Figure 36.

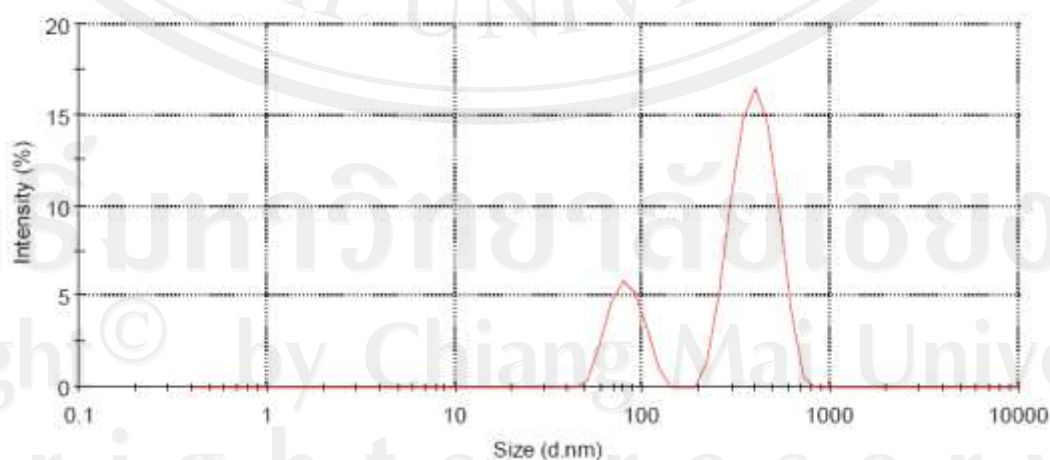


Figure 36 Size distribution of an o/w emulsion containing NLC

In Figure 36, two main peaks are observed, the first one is the peak of NLC and the second one is the peak of oil droplets in the emulsion. However, the performance of using emulsion on hair is lesser than the suspension, because the greasiness effect from the emulsion. From this result, nanosuspension was the most suitable dosage form and will be developed into the hair tonic for determining the hair growth promoting efficacy tested in the C57BL/6 mice model.

Long term physical stability of the hair tonic was checked for 1 year, there were no any changes in the size distribution of the formulation. Comparison of size distribution of the hair tonic is shown in Figure 37. Hair growth promoting efficacy of the hair tonic is shown in Figure 38. Digital images on day 28 of mice received water, minoxidil, blank NLC hair tonic, CT-NLC hair tonic, and safflower extract are shown in Figure 39A, B, C, D, E, respectively.

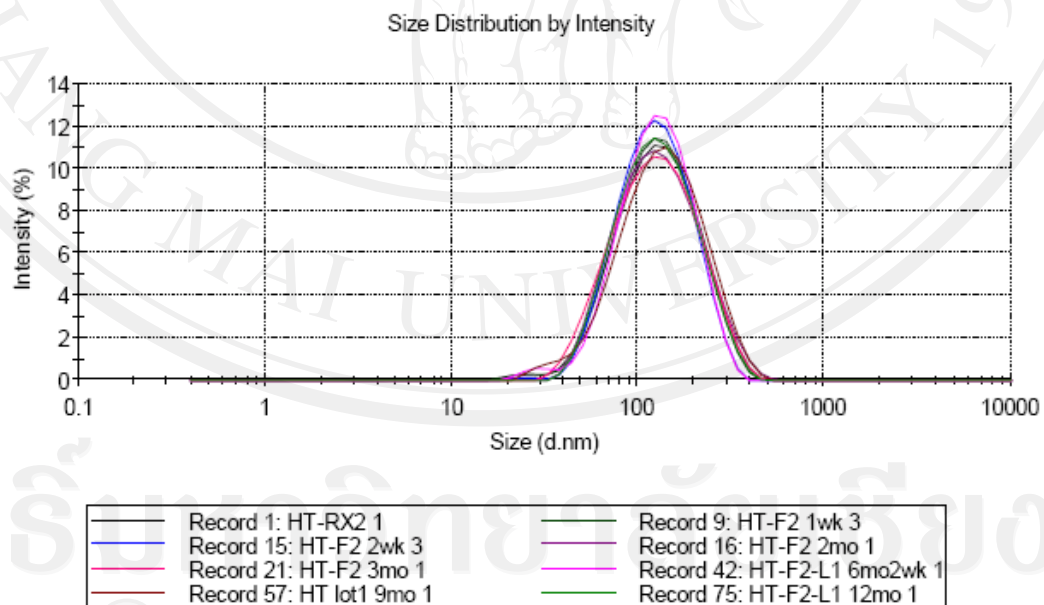


Figure 37 Comparison of size distribution between hair tonic in different time after preparation

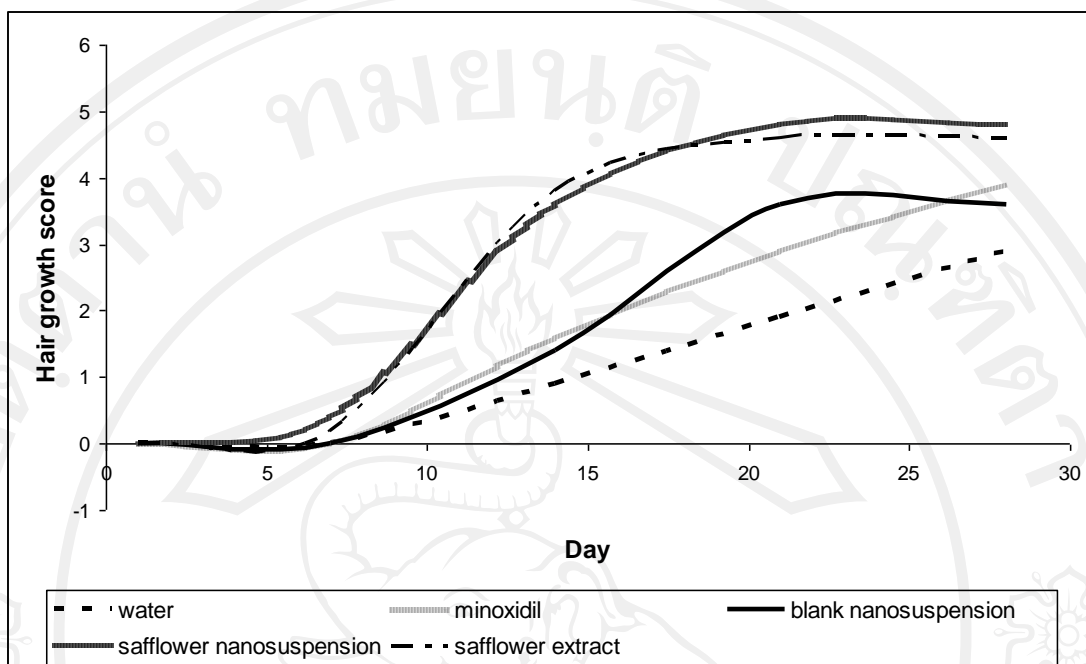


Figure 38 Hair growth promoting efficacy of nanosuspension

As can be seen from Figure 37, hair tonic made from nanosuspension of the NLC F9L1 exerted at least one year stability, since the size distribution of the formulation were not affected by time and there was no statistical different between particle size of the nanosuspension at day 1 and 1 year after being kept at the room temperature.

Batch variations was investigated by preparing three hair tonic products in three different days, there was no significance different in particle size and size distribution between these batches, polydispersity index was used as a parameter for determining the size distribution.

From Figure 38 and 39, there is an interesting in activity of blank nanosuspension which was equal to the minoxidil. This may be a result from intrinsic 5α -reductase inhibitory activity from the lipid material used in the matrix, since it was

known that some fatty acid type molecules can inhibit the enzyme (Liang and Liao, 1992). Safflower nanosuspension showed the greatest hair growth promoting activity, which was not statistical difference from the safflower extract. However, the amount of safflower extract in the CT-NLC was 40-fold diluted than 1% solution of safflower extract. In addition, nanosuspension provided more benefits, for examples, decreasing the safflower extract used, protecting of vulnerable active substance in the safflower. Moreover, physical appearance of nanosuspension was better than the solution of the crude extract.

None of any irritation signs occurred in any mice received blank nanosuspension or safflower nanosuspension.

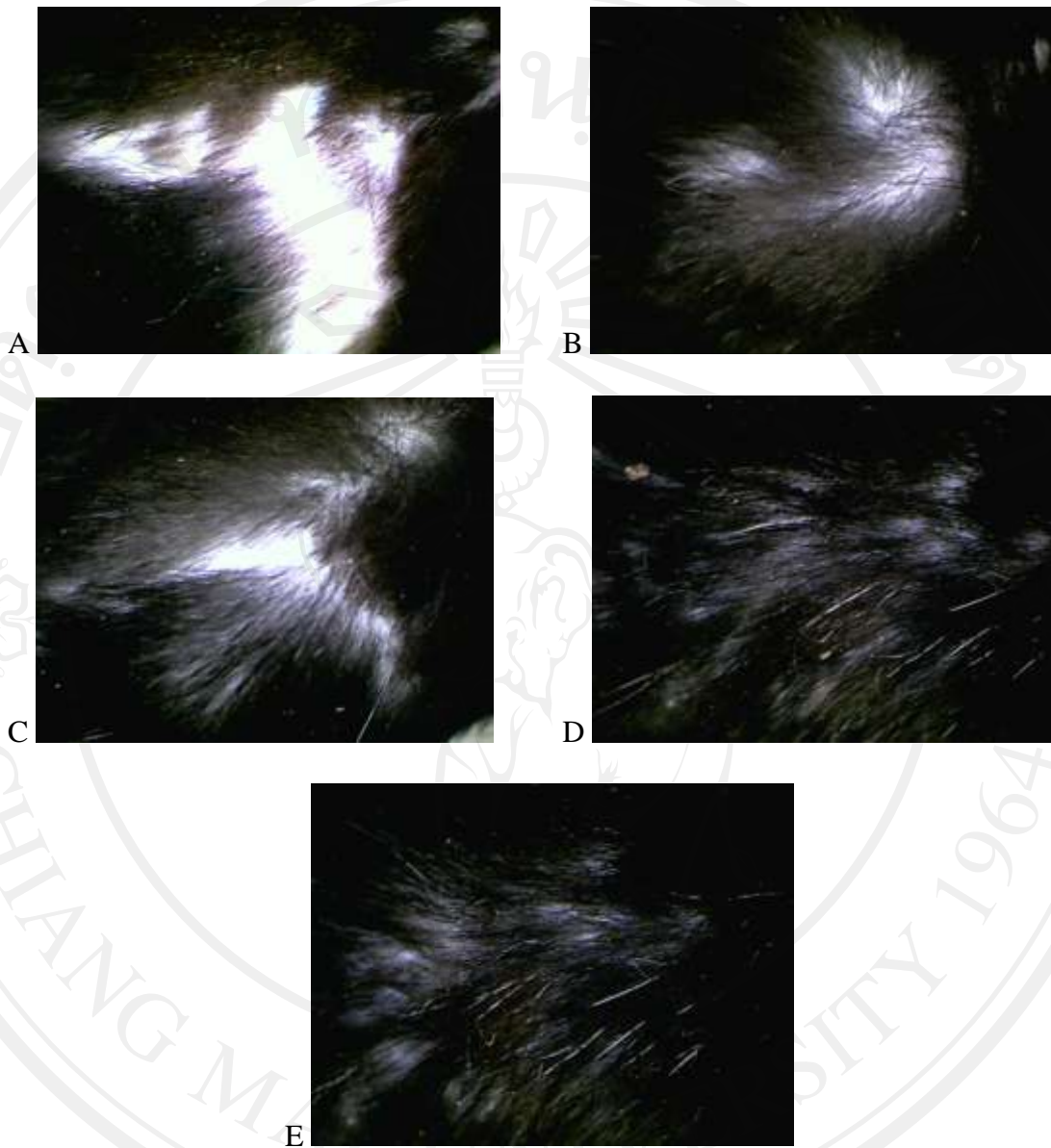


Figure 39 Digital images on Day 28 obtained from Coscam[®] of mice received (A) water, (B) minoxidil, (C) blank NLC hair tonic, (D) CT-NLC hair tonic, and (E) safflower extract.